

# Ion Activation Methods for Peptides and Proteins

Jennifer S. Brodbelt\*

Department of Chemistry, University of Texas at Austin, Austin, Texas 78712, United States

## ■ CONTENTS

Tandem Mass Spectrometry and Proteomics	30
Fragmentation Nomenclature	31
Collisional Activation	32
Electron-Based Activation	33
Photoactivation	34
Other Activation Methods	35
Activation of Deprotonated Peptides	35
Applications for Peptides, Proteins, and Proteomics	37
Large-Scale Evaluation of MS/MS Spectra	37
Data Acquisition Methods	37
Utilizing Multiple Activation Methods	38
Hybrid Activation Methods	39
Separations	40
Top-Down and Middle-Down Methods	40
Native Proteins and Protein Complexes	43
Conclusions	46
Author Information	47
Corresponding Author	47
Notes	47
Biography	47
Acknowledgments	47
References	47

The analysis of peptides and proteins as well as the grander scope of proteomics (large scale study of proteins) has been advanced by the development of a versatile array of ion activation methods that have facilitated characterization of peptides and proteins based on production of diagnostic fragmentation patterns. Improvements of mass spectrometry instrumentation and sample processing methodologies have allowed intensive analysis of complex cell lysates, thus making it possible to identify thousands of proteins in addition to enabling comprehensive characterization of post translational modifications. The successful elucidation of the primary sequence of many peptides and proteins through tandem mass spectrometry has accelerated the development of other complementary methods that support targeted strategies and quantitative approaches and have catalyzed new applications of mass spectrometry in related fields, such as structural biology. This review will describe the development and applications of ion activation methods for peptides and proteins that have played such a critical role in the fields of biochemistry, molecular biology, medicinal chemistry, biotechnology, and structural biology. Moreover, unravelling the fundamental underpinnings of these activation methods have shed light on the factors that influence ion fragmentation upon energization, thus providing predictive insight and motivating new strategies that capitalize on manipulating ion dissociation behavior for specific applications. Given the critical role that tandem mass

spectrometry has played in the field of proteomics and structural biology, this review will emphasize the ion activation methods that have been used to analyze peptides and proteins with an emphasis on new applications over the past 3 years. There are numerous excellent review and tutorial articles that have focused on mass spectrometry-based proteomics technologies, proteomic applications, and specific activation methods in recent years, and thus readers are directed to these to provide additional perspectives.<sup>1–24</sup> In addition, a recent review focused specifically on activation methods in proteomics with an emphasis on characterization of post-translational modifications and tandem mass spectrometry methods for quantitation,<sup>7</sup> so these topics are not covered here. This review opens with some basic tutorial sections to provide background information, followed by more specialized subtopics that demonstrate some of the more recent high impact applications of activation methods for peptides and proteins.

## ■ TANDEM MASS SPECTROMETRY AND PROTEOMICS

Tandem mass spectrometry, known as MS/MS, is one of most versatile and powerful methods for acquiring structural information about a molecule. Although the elemental composition of a peptide can be determined based on highly accurate mass measurement, high mass accuracy alone is not sufficient to assign a sequence or to differentiate peptide isomers which have the same elemental and amino acid compositions. This means that sequence-specific information afforded by MS/MS is indispensable for peptide and protein analysis. The general process of tandem mass spectrometry involves isolation/selection and manipulation (via energization or reaction) of a population of precursor ions and detection of the resulting products. Ion activation, not reaction, is the focus of this review, and in this respect energy can be added in multiple small steps primarily in vibrational modes, as is the case for low energy collisional activation, or in a single fast event, such as absorption of a UV photon. As such, the rate and amount of energy deposition, as well as mechanistic effects, can have significant impact on the outcome for peptides and proteins in terms of the types, abundances, and range of fragment ions produced. For even more structural information, fragment ions can be subsequently activated and dissociated multiples times in a process called MS<sup>n</sup>. There are several general categories of activation methods that have been used for analysis of peptides and proteins, including ones based on collisions with gas molecules or surfaces, interactions with

**Special Issue:** Fundamental and Applied Reviews in Analytical Chemistry 2016

**Published:** December 2, 2015

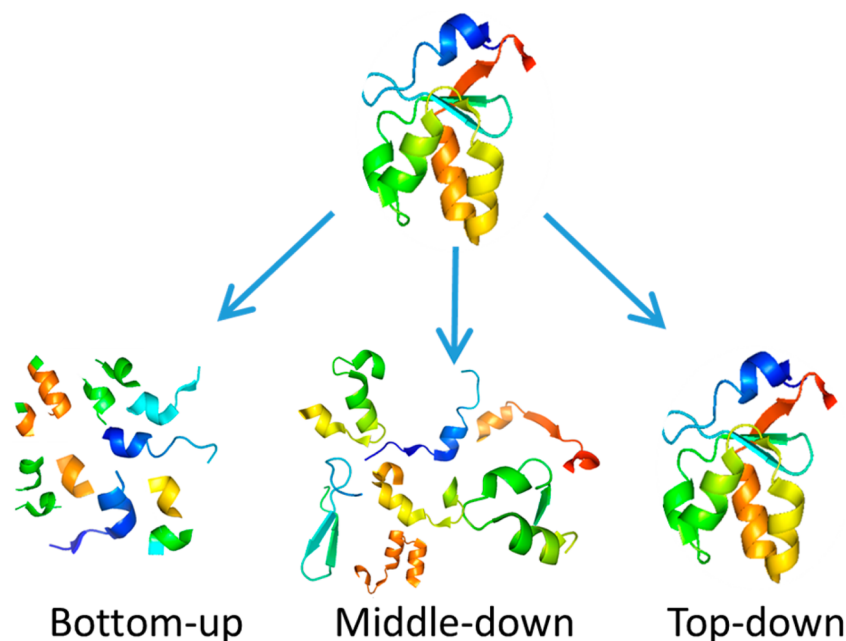


**Figure 1.** Concept of bottom-up, middle-down, and top-down strategies for analysis of proteins.

electrons or electron-donating or electron-accepting reagent ions, or absorption of photons, all of which will be covered in this review, in addition to several emerging methods that may gain popularity as they are more thoroughly developed. Many of these activation methods are complementary to one another, thus providing supporting information when used in a cooperative manner. In fact, no single activation method has proven to be universal for all mass spectrometry platforms and all types of molecules which is why new activation methods continue to be explored and existing methods continue to be refined.

Tandem mass spectrometry has been widely applied for characterization of individual peptides or proteins, in addition to broader, deeper, higher throughput studies for proteomics.<sup>1–24</sup> In the context of mass spectrometry-based proteomics, there are three main approaches: bottom-up, middle-down, and top-down (Figure 1). In the very popular bottom-up approach, proteins are enzymatically digested to produce more readily analyzed peptides that are representative of the original proteins.<sup>1–4</sup> The peptides are typically separated using high-performance liquid chromatography (or other emerging separation methods like capillary electrophoresis), ionized, and activated to create informative fragmentation patterns. Various algorithms are used to assign fragment ions of each peptide which are then matched to proteins. Alternatively, using a top-down approach, proteins are not enzymatically digested but rather are analyzed intact, and intact protein mass measurements are used in combination with the fragmentation patterns generated upon MS/MS to identify the proteins.<sup>19–22</sup> Although protein-level separations and analysis are experimentally challenging, the potential to obtain more detailed information about patterns of post-translational modifications, such as combinatorial patterns that would be lost upon proteolysis of the protein into peptide subunits that are not comprehensively sampled, and conformational information remains a compelling advantage. The intermediate approach is “middle-down” in which proteins are partially proteolyzed prior to analysis resulting in peptides that are larger than

bottom-up peptides and smaller than the intact proteins.<sup>23</sup> This method has been less commonly employed but has gained ground because of the technical difficulties of top-down strategies.

Once fragmentation patterns are generated, there are two primary strategies used to facilitate the identification of peptides and proteins: *in silico* database search methods and *de novo* sequencing.<sup>1,4,25</sup> *In silico* database searches capitalize on the enormous quantity of known genomic sequence information by using sophisticated algorithms to match experimental MS/MS patterns to theoretical tandem mass spectra created *in silico* for peptides from large databases of known proteins. A variety of *in silico* programs have been developed including SEQUEST,<sup>26</sup> Mascot,<sup>27</sup> MassMatrix,<sup>28</sup> OMSSA,<sup>29</sup> X!Tandem,<sup>30</sup> Byonic,<sup>31</sup> and MaxQuant,<sup>32</sup> among others and have proven to be extremely powerful, allowing identification of thousands of proteins in cell lysates. Workflows based on *in silico* algorithms are largely restricted to identification of proteins from organisms with sequenced genomes and predictable modifications. *De novo* sequencing algorithms, in contrast, do not require prior information from a protein database and thus generally obviate the dependence on genomic information.<sup>25,33,34</sup> The *de novo* methods directly interpret fragmentation patterns based on the individual masses and mass differences of the product ions in the mass spectra<sup>33,34</sup> and ultimately provide greater flexibility for identification of unexpected mutations or PTMs. Some of the *de novo* programs developed include PEAKS,<sup>35</sup> PepNovo,<sup>36</sup> NovoHMM,<sup>37</sup> MSnovo,<sup>38</sup> and Vonode,<sup>39</sup> and new emerging ones for intact proteins like Twister.<sup>40</sup>

## ■ FRAGMENTATION NOMENCLATURE

Systematic fragmentation nomenclature has been developed to categorize the types of fragment ions generated by peptides and proteins. Alphabet letters are used to represent categories of fragment ions based on the type of bond cleaved in the peptide or protein backbone, and numbers indicate the position of the cleavage site relative to the N- or C-terminus. The

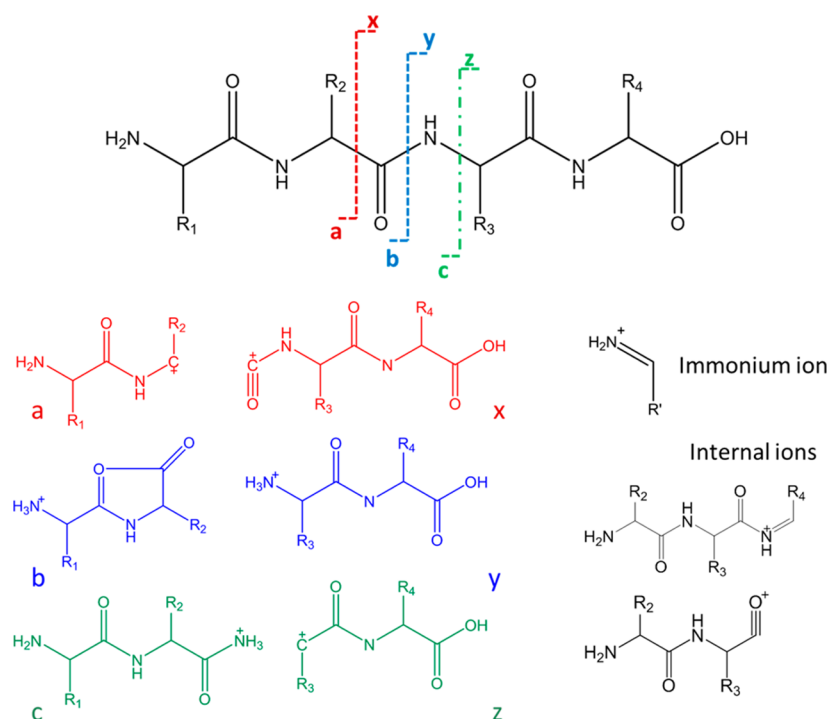


**Figure 2.** Types of fragment ions produced for peptides and proteins.

fragmentation nomenclature of peptides was developed by Roepstorff et al.,<sup>41</sup> as illustrated in Figure 2 for a peptide. For low energy dissociation processes including collision-induced dissociation (CID or collisionally activated dissociation (CAD)) and some types of photodissociation, predominant cleavages of the thermally labile C–N amide bonds of the polypeptide backbone lead to production of b- and y-type ions. Losses of NH<sub>3</sub> or H<sub>2</sub>O and a-type ions (which may arise from the loss of CO<sub>2</sub> from b-type ions) are other common fragment ions from low energy activation. In contrast, electron-based activation methods, such as electron capture dissociation (ECD) and electron transfer dissociation (ETD), generate c- and z-type fragment ions arising from the cleavage of N–C<sub>α</sub> bonds. Higher energy activation methods, such as 193 nm UVPD, generate a/x ions by cleavage of C<sub>α</sub>–C bonds, in addition to b/y and c/z ions. In general, fragment ions that retain the N-terminus of the polypeptide are referred to as a, b, and c-ions, whereas product ions that retain the C-terminus of the polypeptide are labeled as x, y, and z-ions. Complementary ion pairs are a/x, b/y, and c/z ions. Moving along the peptide backbone from the N-terminus to C-terminus, cleavage of the C<sub>α</sub>–C, C–N, and N–C<sub>α</sub> bonds yield a/x, b/y, and c/z ion pairs, respectively. The numerical subscript refers to the number of N-terminal or C-terminal amino acids contained in the product ion. In addition to these ion pairs, internal ions originate from cleavage of multiple backbone bonds or from secondary fragmentation of primary ions during which the characteristic C-terminal or N-terminal portion is lost. Immonium ions are typically low mass ions comprised of single amino acid residues. Product ions that have undergone loss of a side-chain from an amino acid are labeled as d, v, and w ions (depending on whether they are N-terminal or C-terminal ions).

## COLLISIONAL ACTIVATION

After decades of development, widespread implementation on virtually all commercially available tandem mass spectrometers, and countless applications, collisional activation remains the most popular activation method. This method involves energetic collisions between ions of interest and nonreactive gas atoms, typically helium, nitrogen, or argon, in which some portion of the kinetic energy of the ion is converted to internal energy upon each activating collision.<sup>42</sup> Ultimately, the accumulation of internal energy in the ions leads to their dissociation. The high efficiency of most collisional activation methods is an enormous advantage that makes it a top choice for many proteomics applications, and it is a routine feature of virtually all tandem mass spectrometry platforms (Q-TOF, triple quadrupole, ion traps, FTICR, etc.). Perhaps the main disadvantage of low energy collisional activation methods is that energy deposition typically occurs via a stepwise, multicollision process which tends to limit the total energy deposition and favors fragmentation via lower energy pathways. This shortcoming of collisional activation results in cleavage of the most labile bonds and frequently causes structurally uninformative neutral losses such as water, ammonia, or CO<sub>2</sub> for peptides and proteins.<sup>43,44</sup> An additional shortcoming of conventional low energy CID in ion trap instruments arises from truncation of the lower *m/z* range that results from the adjustment of the radiofrequency trapping voltage during ion activation to ensure adequate ion energization. This prevalent problem, often termed the low mass cutoff (LMCO), has proven detrimental to detection of shorter N-terminal and C-terminal fragment ions of peptides. This limitation was largely alleviated by the development of higher energy collisional activation dissociation (HCD) in ion traps,<sup>45</sup> now enabled on most commercial ion trap platforms. HCD is implemented by accelerating the ions of interest in a separate collision cell or multipole as a means of beam-type collisional activation (akin to the way that collision activation is performed on triple

quadrupole systems). Because the activation process is independent of the trapping parameters, the lower mass range is not truncated. At the same time, energy deposition is typically higher for HCD compared to conventional CID in an ion trap mass spectrometer.

To date, CID remains the “gold standard” to which all other ion activation methods are compared. Much of the dominance of CID in the field of proteomics stems from its robust performance as well as its increasingly well-understood underpinnings.<sup>43,44</sup> In particular, the mobile proton model has provided a framework for understanding fragmentation pathways observed for protonated peptides upon CID,<sup>46,47</sup> and the complementary pathways in competition model has supplied a more detailed energetic and kinetic depiction of peptide fragmentation.<sup>43</sup> The mobile proton model assumes that ionizing protons are initially located at basic sites such as the N-terminus or side-chains of lysine, arginine, and histidine. Upon collisional activation, one or more of the ionizing proton(s) may migrate to less basic sites of the polypeptide which facilitates various charge-site-initiated mechanisms of backbone cleavage. In particular, a mobile proton can produce N-protonation of the amide bond which precedes cleavage of the amide bond to yield diagnostic b- and y-ions. Nonspecific cleavages associated with the mobile proton model typically occur when there are more charging protons (e.g., a higher charge state) than the number of very basic sites, particularly charge-sequestering arginine. Preferential sequence-specific backbone cleavages can restrict the information obtained from peptides containing proline and aspartic acid residues.<sup>46,47</sup>

For example, proline-containing peptides and proteins exhibit enhanced cleavage of the amide bond N-terminal to the proline residues, an outcome that is especially exacerbated for ions in higher charge states (with more mobile protons). For peptides and proteins in low charge states (lacking mobile protons), preferential cleavage of the amide bond located C-terminal to acidic residues is also common. The combination of these effects can limit the extent of fragmentation for those peptides or proteins containing multiple proline and aspartic acid residues. Another shortcoming of CID arises from the lability of PTMs such as phosphorylation<sup>43</sup> because many types of collisional activation are slow heating methods, thus the weakest bonds are predominantly cleaved. This is manifested as neutral losses of PTMs, an outcome that limits the utility of CID for site localization of PTMs.

## ■ ELECTRON-BASED ACTIVATION

Electron-based dissociation methods, such as electron capture dissociation (ECD)<sup>48–50</sup> and electron transfer dissociation (ETD),<sup>51,52</sup> have gained widespread use in the past decade for the analysis of peptides and proteins. ECD entails the interaction of positively multicharged analyte ions with low energy electrons, leading to capture of electrons in an exothermic process that leads to charge reduction and fragmentation.<sup>8,9,49,50</sup> ECD is typically performed within the magnetic field of FTICR mass spectrometers where electrons and analyte cations can be trapped simultaneously. Although ECD has been widely and successfully used in FTICR mass spectrometers, it proved difficult to implement in quadrupole ion traps because the necessary thermal electrons could not be suitably trapped in the dynamic fields created by application of radiofrequency voltages. An alternative ECD-like method, called electron transfer dissociation (ETD), was developed and implemented on ion trap instruments.<sup>51,52</sup> For ETD,

positively charged analyte ions react with radical anions, thus causing an electron to be transferred.<sup>10–14</sup> Capture of a low-energy electron (e.g., ECD) or the transfer of an electron during an ion/ion reaction (e.g., ETD) is thought to proceed through the capture/transfer of an electron at the site of an ionizing proton via an exothermic process that induces backbone cleavage through the migration of a hydrogen radical. The mechanism of ECD has been investigated extensively.<sup>53–55</sup> The capture of a low energy electron ultimately results in formation of an odd-electron radical species and generally with little vibrational energy redistribution prior to cleavage of a N–C<sub>α</sub> backbone bond. Whether produced by ETD or ECD, the resulting charge-reduced ions may undergo subsequent fragmentation at the N–C<sub>α</sub> bond, generating c- and z-type fragment ions rather than the b- and y-type ions that are commonly produced by CID. Rearrangement and transfer of  $\alpha$ -carbon radicals to backbone carbonyls, initiating a free radical reaction cascade, may also occur during ECD and ETD, ultimately resulting in fragment ions that may differ in the hydrogen atom content.

Other electron-based activation processes have been reported, although none have reached the widespread popularity of ECD and ETD. Electron induced dissociation (EID) involves the interaction of singly protonated peptides with moderately low energy electrons, resulting in radical ions that dissociate.<sup>56–58</sup> The interaction of multiprotonated peptides with >20 eV electrons results in ionization and electronic excitation of the peptides in a process known as electron ionization dissociation (also known as EID).<sup>59</sup> The resulting radical ions may undergo spontaneous fragmentation via side-chain losses and backbone fragmentation, predominantly via C–C cleavage to product a/x ions and N–C<sub>α</sub> cleavage to generate c/z ions.

Electron-based methods have demonstrated several compelling advantages for activation of peptides and proteins.<sup>8–14</sup> First, electron-based methods do not cause the loss of post-translational modifications and thus can be used to localize sites of modifications. Although both ECD and ETD have been very useful for characterization of peptides and proteins, both of these methods show a significant dependence on charge states of the precursor ions. As electron transfer is necessary prior to dissociation, these electron-based activation methods are not suited for singly protonated precursors and are more efficient for higher multiply charged precursors (3+, 4+, 5+, etc.). Ions in low charge state ions tend to undergo charge reduction rather than dissociation (e.g., ETnD), producing few fragment ions instead of diagnostic complementary c- and z-type fragment ions. For peptide ions in low charge states, especially for doubly charged ions, it has been shown that intramolecular interactions were retained in some cases after electron activation, thus impeding disassembly of the resulting fragment ions. Several means to enhance radical mobility and disrupt intramolecular interaction are now commonly employed, including supplemental collisional activation or infrared photoexcitation, both of which cause heating of the radical ions and enhance the separation (disassembly) of the fragment ions from each other.<sup>60–64</sup> The use of low level collisional activation or infrared photoactivation, prior to or during the ECD/ETD process, is termed activated-ion ECD/ETD.<sup>60–64</sup> The addition of extra internal energy effectively disrupts peptide/protein secondary and tertiary structure and allows more effective generation and detection of ECD/ETD products. ECD and ETD methods have proven to be especially useful for analysis

of intact proteins, in part because of the more “random” nature of electron activation which promotes cleavages deeper into the midsection of the protein sequences than conventional collisional activation methods.<sup>9,14,65–68</sup> In addition, the high charge states of proteins are well-suited for electron-based activation.

Other related or specialized electron-based methods for peptide anions have also emerged, including electron detachment dissociation (EDD),<sup>69–72</sup> negative ion electron capture dissociation (niECD),<sup>73–75</sup> and negative electron transfer dissociation (NETD),<sup>76–81</sup> all generally geared for deprotonated species. Activation methods specifically developed for deprotonated peptides are discussed in a later section.

## ■ PHOTOACTIVATION

Absorption of photons by gas-phase ions leads to energization that can result in fragmentation, hence the term photodissociation.<sup>16–18</sup> Photodissociation offers several interesting features or advantages as an ion activation method. Photoactivation methods offer selectivity and tunability depending on the type of laser used. Using pulsed lasers also provides the benefit of very fast (e.g., nanosecond) activation periods because of short nanosecond pulse widths. Using high energy photons, such as in the UV range, results in high energy deposition per photon and thus translates into a greater array of fragment ions.<sup>16–18</sup> For example, photoexcitation using 157 or 193 nm photons accesses excited electronic states, thus opening new fragmentation pathways of peptides or proteins.

The number of photons needed to induce dissociation is dependent on the photon wavelength and can range from several hundred photons in the IR range ( $\sim 0.1$  eV per photon) to a single UV photon ( $\sim 3$ – $8$  eV per photon). One of the original types of photodissociation involved irradiation of ions by a high flux of low energy infrared photons, typically from a CO<sub>2</sub> (10.6  $\mu$ m) laser. This wavelength is efficiently absorbed by various vibrational modes associated with C–C, C–N, and P–O bonds of molecules. Because of the very low energy per photon ( $\sim 0.1$  eV), accumulation of multiple photons is required for fragmentation of ions.<sup>82</sup> The activation process of infrared multiphoton dissociation (IRMPD) is akin to the thermal heating process of low energy CID, thus resulting in cleavage of the most labile bonds of peptides. IRMPD has been most successful in FTICR mass spectrometers because these instruments operate at extremely low pressure so that collisional cooling of ions does not compete with photodissociation. IRMPD is also suitable for QIT instruments because the ions can be trapped and irradiated for many milliseconds to allow sufficient accumulation of energy, although in competition with deactivation of ions via collisional cooling that occurs in QITs.<sup>82</sup> Despite IRMPD being particularly effective for analysis of phosphopeptides owing to the high IR photoabsorption cross sections of P–O stretching modes, it has rarely out-performed conventional CID methods and thus has not gained sweeping popularity for proteomics applications.<sup>83–85</sup>

In contrast to IRMPD, ultraviolet photodissociation (UVPD) uses higher energy ultraviolet photons to activate and dissociate ions. Successful UVPD of peptides has been demonstrated using a variety of lasers, including F<sub>2</sub> excimer laser (157 nm, 7.9 eV per photon),<sup>86</sup> ArF excimer laser (193 nm, 6.4 eV per photon),<sup>87</sup> a femtosecond titanium sapphire laser (800 nm, 1.5 eV per photon),<sup>88</sup> a Nd:YAG laser (266 nm, 4.7 eV per photon<sup>89–91</sup> or 355 nm, 3.5 eV per photon<sup>92</sup>), and a XeF

excimer laser (351 nm, 3.5 eV per photon).<sup>93</sup> (Photodissociation has also been implemented using visible photon wavelengths, such as 473 nm.)<sup>94,95</sup> For each wavelength, UVPD requires a suitable chromophore for absorption of photons. UVPD has most commonly been performed using 157 or 193 nm photons generated by F<sub>2</sub> or ArF excimer lasers, respectively. Of these two wavelengths, 193 nm has been more prevalent because there is only a small loss when transmitting through air and common fused silica optics can be used. For ultraviolet and visible lasers with photon energies between 3 and 8 eV ( $\sim 400$ – $150$  nm), one or two photons provide enough energy to cause transition of ions to excited electronic states. Dissociation may occur directly from the excited states, an opportunity that largely accounts for the broad diversity of fragmentation pathways observed upon UVPD.<sup>86,96–101</sup> Alternatively, ions may undergo internal conversion and intramolecular vibrational redistribution that may lead to product ions of the type more commonly observed upon collisional activation. Reilly's group, in particular, has undertaken the most extensive studies to elucidate UVPD mechanisms and pathways, thus justifying that UVPD entails photolytic radical cleavage of the C–C <sub>$\alpha$</sub>  bond prior to radical elimination to form a/x-type ions and other subsequent products.<sup>86,96–100</sup>

The absorption spectrum of polyaniline in the vacuum ultraviolet range displays three bands centered at approximately 190, 160, and 130 nm, bands assigned to transitions involving the amide bond of the polypeptide backbone.<sup>102</sup> Given this photoabsorption behavior, 157 and 193 nm wavelengths are particularly versatile for activation of peptides and proteins because these photons are absorbed by amide bonds meaning that the entire backbone may serve as a chromophore. Each photon carries a large amount of energy (7.9 and 6.4 eV, respectively), thus exciting proteins and peptides into higher electronic states. This allows access to diverse fragmentation pathways, including ones with higher activation energies. The resulting product ions from this type of UVPD span all six fragment types (a, b, c, x, y, and z), among others. Several studies have focused on UVPD of singly charged peptides, ones with N- or C-terminal arginine residues (sequestered ionizing protons) to mimic peptides generated by trypsin digestion.<sup>96–100</sup> These experiments yielded ions predominantly from the terminus that contained the charge.<sup>96–100</sup> When the peptides contained a lysine residue instead of an arginine, the proton was more mobile which led to competitive fragmentation pathways, such as formation of c/z and b/y ions, in addition to homolytic cleavage of the C <sub>$\alpha$</sub> –C bond to form a/x ions. The broad array of product ions produced by UVPD yields extensive sequence coverage and has afforded confident identification of peptides while maintaining labile PTMs. UVPD (193 nm) has been utilized in a number of proteomic applications,<sup>103–122</sup> including ones aimed at characterization of sites of modifications, including phosphorylation,<sup>104,105</sup> sulfation,<sup>106–108</sup> and glycosylation,<sup>1,109,110</sup> for de novo sequencing<sup>111</sup> and for extending the breadth and depth of bottom-up methods via evaluation of acidic peptides in the negative mode.<sup>112,113</sup> UVPD (193 nm) has also shown success for analysis of intact proteins and protein complexes,<sup>116–122</sup> both discussed in more detail in later sections.

A 266 nm photon delivers 4.7 eV of energy and can lead to production of a, b, c, x, y, and z ions upon absorption by a peptide.<sup>1,123–131</sup> The aromatic side-chains of tryptophan, phenylalanine, and tyrosine absorb around 260–270 nm, allowing absorption of this range of wavelengths by peptides

and proteins containing these amino acids. One particularly unique characteristic of 266 nm UVPD is that peptides or proteins containing disulfide bonds exhibit a homolytic cleavage of the disulfide bonds.<sup>126</sup> Another strategy that exploited the selective absorption of 266 nm photons entailed iodination of tyrosine residues.<sup>125,127–130</sup> Exposure of the iodinated peptides prior to 266 nm photons promoted radical directed dissociation which has proven useful in several peptide/protein applications, including probing gas-phase protein structure,<sup>128,130</sup> pinpointing phosphorylation sites,<sup>125</sup> and differentiating between D- and L-amino acids in peptides.<sup>127,129</sup>

Using wavelengths in the range of 350 nm is counterintuitive because peptides and proteins do not absorb in this range, but it provides another opportunity to selectively target molecules based on tagging with appropriate chromophores. This wavelength range is produced by an XeF excimer laser (351 nm)<sup>132–135</sup> and the third harmonic of a Nd:YAG laser (355 nm).<sup>92</sup> After incorporation of chromophores, the resulting chromophore-modified peptides absorb upon exposure to ~350 nm photons and produce b/y ions similar to collisional methods (not the greater range of fragment ion types typically produced by vacuum UV or higher energy UV photons). This chromophore-tagging strategy combined with 351 nm (or 355 nm) UVPD has been explored in several recent applications. For example, one strategy integrated AlexaFluor 350, a cysteine selective chromophore probe with a high photoabsorption cross section at 350 nm, with 351 nm UVPD to target heavy chain complementary determining regions (CDR) of immunoglobulin G.<sup>132</sup> After tagging the CDRs with AlexaFluor 350 (a commercially available dye), 351 nm UVPD-MS provided a facile way to identify and differentiate cysteine-containing antigen binding regions from other redundant peptide sequences.<sup>132</sup> Pairing chromophore-tagging methods with 351 nm UVPD has been reported for other applications, such as addressing the challenge of high-throughput bottom-up analysis of complex mixtures by selectively tagging specific residues, like histidine and tyrosine, via a diazonium labeling reaction.<sup>135</sup> Diagnostic fragmentation patterns were produced only for the tagged peptides upon UVPD, thus reducing the redundancy of database searches.<sup>135</sup> In another application, the conformations of proteins were evaluated using 351 nm UVPD in conjunction with a chromogenic chemical probe. The probe reacted with primary amines (N-terminus and lysine side-chains) in a manner that was dependent on the relative solvent accessibility (e.g., exposure) of each amino acid in the protein in a native solution environment.<sup>93,133</sup> The chromophore-tagged peptides could be readily differentiated from unlabeled peptides based on UVPD, thus streamlining the mapping of solvent accessibility of proteins.<sup>93,133</sup> UVPD using 351 nm photons has also been used to facilitate de novo sequencing methods. On the basis of tagging all proteolytic peptides at their N-termini with a UV chromophore and exposing the peptides to multiple UV pulses, the resulting MS/MS spectra contained a clean series of y-type ions.<sup>134</sup> This method alleviated misassignments of peptides because of the difficulties in differentiating b- and y-type ions commonly formed by conventional collisional activation methods.

## ■ OTHER ACTIVATION METHODS

In the ongoing exploration of ion activation, various other activation methods have been developed, each offering particular advantages and unique applications. For example,

surface induced dissociation (SID) generates fragment ions upon collision of precursor ions with a surface which represents a pseudoinfinite mass target.<sup>136,137</sup> Collisions with a surface cause high energy deposition and extensive peptide fragmentation.<sup>136,137</sup> SID results in formation of CID-like product ions (b- and y- fragments) of peptides and gives comparable sequence coverage to that observed with CID. In more recent years, it has largely been used to disassemble protein complexes,<sup>138–144</sup> as discussed in a later section; SID has not been adopted for high-throughput proteomics.

Other methods have used high energy projectiles to promote activation and dissociation of peptides.<sup>145–151</sup> For metastable atom-activated dissociation (MAD), a keV beam of helium metastable atoms interacts with protonated peptides via a combination of Penning ionization and charge reduction processes that result in fragmentation of the peptide backbone, leading to formation of a/x, b/y, and c/z ions.<sup>147–149</sup> Charge transfer dissociation (CTD) uses keV helium cations to cause ionization of protonated peptides, and the exothermicity of the resulting electron abstraction process results in fragmentation of the peptides.<sup>150</sup> The products are ones that arise from cleavage of the C–C<sub>α</sub> backbone bond of peptides, leading to formation of a-type ion.<sup>150</sup> Complementary x ions were not observed, an outcome rationalized because the targeted peptides had a basic residue at the N-terminus.<sup>150</sup> In addition to a ions, a + 1 ions (i.e., fragment ions with one more hydrogen atom than a ions) were produced, thus confirming that radical mechanisms were operative upon interaction of the peptides with the high energy helium ions.<sup>150</sup> A microwave plasma source was interfaced to an Orbitrap mass spectrometer to generate a high energy beam (1–2 keV) of air cations that interacted with peptide ions.<sup>151</sup> These high energy reactions and dissociation processes resulted in charge reduction and backbone cleavages.<sup>151</sup> Although the fragmentation was relatively inefficient, a range of fragment ions, including a/x, b/z, and c/y ions, were generated.<sup>151</sup> None of these projectile-based methods has yet to reach mainstream adoption. These strategies demonstrate that innovative activation methods continue to be discovered and may lead to future breakthroughs for characterization of peptides and proteins.

## ■ ACTIVATION OF DEPROTONATED PEPTIDES

The outstanding performance of activation methods for protonated peptides and proteins and the mature database search algorithms that have been developed for large scale proteomics applications explain why the positive ionization mode has been used for most MS/MS studies of peptides and proteins. However, the negative mode offers intriguing opportunities to extend the range of proteomics studies for specialty or niche applications. For example, certain classes of peptides and proteins with numerous acidic amino acids or acidic post-translational modifications may more readily ionize in the negative mode and in fact may be easier to detect in the presence of confounding interferences that may dominate spectra acquired in the positive mode. As a consequence, there has been interest in developing and exploring activation methods well suited for peptide anions.

Collisional activation is often not as effective for analysis of deprotonated peptides compared to protonated peptides; rather the resulting fragmentation patterns are typically dominated by uninformative neutral losses (CO<sub>2</sub>, H<sub>2</sub>O, and phosphate groups) and less frequent backbone cleavages. Electron activation and UV photoactivation methods have

demonstrated greater success for peptide anions, resulting in predictable fragmentation arising from the  $C_{\alpha}$ -C bond cleavages (formation of a- and x-type sequence ions). Activation methods geared for deprotonated peptides include electron detachment dissociation (EDD),<sup>69–72</sup> negative electron transfer dissociation (NETD),<sup>76–81</sup> electron photodetachment (EPD),<sup>152–154</sup> and UVPD.<sup>105–113,155</sup>

EDD involves the interaction of moderately high energy electrons ( $\geq 10$  eV) with multideprotonated peptides, causing electron detachment from the peptide.<sup>69–72</sup> The net result is exothermic charge reduction of the peptide that is accompanied primarily by cleavage of  $C_{\alpha}$ -C bonds to produce a/x ions in addition to some c- and z-type ions.<sup>69–72</sup> EDD does not cause disruption of post-translational modifications, making it possible to map sulfonation and phosphorylation sites of acidic peptides.<sup>71</sup>

UVPD can also be readily implemented in the negative mode because photoabsorption is independent of the polarity of the peptide ion.<sup>105–113,152–155</sup> Similar to the EDD and NETD, UVPD of deprotonated peptides results in predictable and consistent formation of a/x ions.<sup>105–113</sup> Electron photodetachment dissociation (EPD) is similar to EDD with the exception that absorption of a UV photon by a deprotonated peptide results in electron detachment.<sup>152</sup> The resulting charge-reduced precursors frequently do not spontaneously dissociate, and thus subsequent collisional activation of the charge-reduced photodetachment species facilitates the formation of product ions via cleavage of  $C_{\alpha}$ -C bonds to produce a/x ions.<sup>153</sup> These products are the same type observed upon EDD but with greater opportunity for radical migration that increases the diversity of fragment ions for EPD.<sup>152</sup> A similar process promoted by UV irradiation of peptide anions is termed activated electron photodetachment (a-EPD), a two-step process in which UV photoactivation using 262 nm photons is used to produce charge-reduced peptide radicals prior to collisional activation.<sup>153</sup> In one systematic comparative study, EDD and a-EPD were evaluated in parallel for characterization of peptide anions. Cleavages next to negative charge solvation sites on the backbone were preferential for EDD, whereas cleavages adjacent to aromatic (tryptophan, tyrosine) and histidine residues were dominant for EPD.<sup>154</sup>

Another electron-based activation method, negative ion electron capture dissociation (niECD), entails the capture of an electron (3–7 eV) by a deprotonated peptide, resulting in an increase in the net charge of the peptide and formation of c/z ions.<sup>74,75</sup> Similar to most other electron activation methods, the process of niECD does not disrupt post-translational modifications and thus can be a viable option for characterization of modified peptides like phosphopeptides and sulfopeptides.<sup>75</sup>

NETD is another analogue to EDD with the exception that electron-deficient reagent cations are used to extract an electron from the deprotonated peptides (rather than using reactions with electrons to dislodge electrons).<sup>76–81</sup> The transfer of an electron from the peptide to the reagent is an exothermic reaction that results in production of a and x ions. Several reagents, including xenon cations and fluoranthene cations, have primarily been used for NETD. A comparison of these two reagents indicated that xenon cations resulted in a greater portion of uninformative neutral losses and more complicated spectra overall relative to NETD using reactive ions from fluoranthene.<sup>77</sup>

Among all the proteomic studies undertaken in the negative mode, the most extensive ones have utilized NETD<sup>76–81</sup> or NUVPD.<sup>105–113</sup> One investigation reported the trends for side-chain losses upon NETD of a wide array of deprotonated peptides,<sup>78</sup> ultimately identifying 19 characteristic neutral losses related to 17 amino acids or modified amino acids. A follow-up study reported the use of NETD to characterize the most acidic portion of the *S. cerevisiae* proteome.<sup>79</sup> For the latter study, NETD enabled on a high performance Orbitrap mass spectrometer resulting in identification of over 2 000 peptides from a combination of GluC and trypsin digests of yeast and allowed identification of many unique acidic peptides that were not found using a more conventional positive mode workflow.<sup>79</sup>

Activated ion NETD (AI-NETD) was implemented as a means of improving the metrics of NETD, especially for peptides in lower charge states.<sup>80</sup> Both supplemental collisional activation and infrared photoactivation were used to enhance peptide dissociation, and although neither method afforded a significant improvement in fragmentation efficiency, both enhanced the formation of diagnostic sequence ions in terms of sequence coverages, often by a factor of 2–5.<sup>80</sup> AI-NETD was recently used for an extensive study of the yeast proteome (*Saccharomyces cerevisiae*), and the improvements in NETD performance by the addition of the infrared photoirradiation during the entire NETD reaction period led to a significant gain in performance.<sup>81</sup> Over 1 000 proteins were identified based on the analysis of tryptic or LysC peptides and over 850 proteins were identified based on GluC peptides.<sup>81</sup>

A high throughput study using UVPD for activation and dissociation of peptide anions was reported for the *Halobacterium* and HeLa proteomes.<sup>112</sup> The large-scale study entailed statistical validation of a database search algorithm (MassMatrix) for automated analysis of negative polarity UVPD mass spectra. On the basis of LC-negative mode UVPD analysis of tryptic digests of *Halobacterium salinarum* and HeLa cell lysates, 3 663 and 2 350 peptides were identified for the *Halobacterium* and HeLa tryptic digests, respectively.<sup>112</sup> Over 800 protein were identified for the *Halobacterium* proteome and over 600 proteins were identified for the HeLa samples, in each case with approximately 50 unique proteins not identified by conventional MS/MS methods. UVPD by itself led to the identification of 68% of the 1181 proteins found for the *Halobacterium* samples.<sup>112</sup> In this same study, a workflow that utilized alternative positive and negative mode scans (i.e., polarity switching) in the same chromatographic elutions was implemented to facilitate identification of both the most basic and more acidic peptides.

A systematic comparison of UVPD and NETD for deprotonated peptides indicated that UVPD outperformed NETD for lower charge states ( $n \leq 2$ ) in terms of the number of diagnostic sequence ions, but both methods were comparable for higher charge states.<sup>155</sup> Sequence coverages averaged 100% for UVPD and 60% for NETD for typical peptides. One notable advantage of UVPD was the significantly shorter activation (<5 ms) compared to typically ~200 ms for the NETD reaction period. UVPD resulted in a more elaborate series of products (b-, y-, c-, z-, Y-, d-, and w-type ions as well as a- and x-type ions), whereas NETD typically produced mainly a/x-type ions.<sup>155</sup> For the broadest sampling of the proteome, integration of positive mode and negative mode MS/MS data offered the best option.

## ■ APPLICATIONS FOR PEPTIDES, PROTEINS, AND PROTEOMICS

The deep fundamental understanding of collisional activation of protonated peptides has accelerated development of increasingly sophisticated predictive algorithms for peptide fragmentation and inspired the use of collisional activation as the MS/MS method of choice for countless bottom-up proteomics applications.<sup>1–4</sup> The success of collisional activation methods, as well as uncovering its shortcomings, motivated the exploration and development of alternative activation methods for peptides, proteins, and large scale proteomics applications.<sup>7–18</sup> Cataloging the numerous studies that have reported extremely impressive performance metrics of bottom-up proteomics workflows based on CID, as well as ETD and UVPD, is beyond the scope of this review, and the reader is instead directed to several recent proteomics/MS reviews.<sup>1–14</sup> Specific notable developments in the arena of proteomics, particularly ones which showcase the impact of powerful ion activation methods, are described in the following sections because they demonstrate the scope of advances in the field of ion activation.

**Large-Scale Evaluation of MS/MS Spectra.** Understanding the fragmentation patterns produced upon energization of ions using any of the various activation methods improves the ability to interpret the spectra, develop mechanistic insight, and incorporate the resulting information into algorithms to identify peptides and proteins. Systematic and deep studies of large data sets of HCD (beam-type CID on ion trap systems) spectra<sup>156,157</sup> have recently provided the type of insight about fragmentation trends of peptides that have previously been documented for low-energy CID spectra obtained on triple quadrupole, QTOF, and ion trap platforms in the prior decade.<sup>158–160</sup> The types of preferential cleavages observed upon conventional low energy CID were previously described above, including cleavage of the amide bonds N-terminal to proline and C-terminal to aspartic and glutamic acid. HCD-MS studies, typically entailing statistical analysis of thousands of peptides according to charge state and size of peptide, have shown that the formation of extensive arrays of *y*-ions, in addition to less frequent and shorter *b* ions, are the most diagnostic products in HCD spectra of tryptic peptides.<sup>156,157</sup> Moreover, internal ions, while often less informative or even unassignable, are common throughout the spectra, and both immonium ions and side-chain fragments are prevalent in the low *m/z* region of the spectra.<sup>156,157</sup> In comparison to CID, HCD produced shorter *y* ions in lower charge states and some of the preferential cleavages commonly observed for CID were modulated for HCD. For example, N-terminal backbone cleavages adjacent to amino acids with hydrophobic residues (I, L, V, F, Y, W) were substantially enhanced for HCD.<sup>156,157</sup>

Large-scale analysis of ECD and ETD spectra have also been undertaken using statistical data mining methods in order to assist in the interpretation of spectra.<sup>161–165</sup> The most extensive study entailed examination of nearly 12 000 peptides created from LysC digestion, over 12 000 peptides produced by Glu-C digestion and over 6400 peptides from trypsin digestion.<sup>163</sup> Although preferential cleavages were not as significantly enhanced as observed upon collisional activation of peptides, some selective cleavages correlated with charge state and amino acid composition of the peptides. For example, it was found that the abundances of *c*-type fragment ions generally increased

with the length of the *c* ion, and backbone cleavages increased C-terminal to E, H, N, Q, R, and W residues and were suppressed N-terminal to G, I, and V residues.<sup>163</sup> These preferential cleavages were less notable for more highly charged peptides. In general, ETD of doubly charged tryptic peptides resulted in predominant formation of C-terminal ions (typically *z* ions) because of the localization of the single remaining charge (after electron attachment) at the basic Arg or Lys residue located at the C-terminus of tryptic peptides.<sup>163</sup>

Analogous to the deep statistical studies undertaken to analyze fragmentation trends of peptides subjected to collisional activation, similar types of large scale investigations have been performed for UVPD data sets.<sup>112,166</sup> The UVPD mass spectra of 1345 arginine-terminated peptides were examined, all with Arg at the C-terminus to mimic tryptic peptides.<sup>166</sup> Numerous *b/y* and *a/x* products from backbone cleavages were identified, as well as *v* and *w* ions (side-chain loss products from *x* ions), internal ions, and immonium ions characteristic of high energy activation. It was found that certain *v*-type ions facilitated confirmation of the N-terminal amino acids of the peptides.<sup>166</sup> Evaluation of the UVPD mass spectra of nearly 6 000 deprotonated tryptic peptides showed that *a/x* ions were the primary types of fragment ions, along with lower frequencies of *y*, *z*, *a + 1*, *x + 1*, and *a + 2* ions (with the latter mass shifted by 1 or 2 Da from hydrogen atom migrations).<sup>112</sup>

**Data Acquisition Methods.** Innovative automated data acquisition approaches have greatly facilitated the collection of MS/MS spectra in a high-throughput manner.<sup>167</sup> In particular, data-dependent and both data-independent and multiplexed workflows have been developed, with each exploiting the tremendous capabilities of ion activation strategies to maximize information content of bottom-up proteomics applications.<sup>168</sup> The approach with the longest track record is data-dependent acquisition (DDA), in which precursor ions are selected and analyzed based on their abundance or signal-to-noise in an initial MS1 spectrum.<sup>169</sup> The DDA method effectively streamlined analysis time and allowed collection of MS/MS spectra for uninformative species to be minimized.<sup>169</sup> Newer methods have coupled DDA with exclusion lists that prevented high abundance precursors from repeated selection and analysis in subsequent scans.<sup>170</sup> Although widely utilized, the DDA methods relied on collection of MS/MS spectra in a serial manner for different precursors and were largely based on selection and activation of the most abundant precursor peptides. Targeted methods include selected reaction monitoring (SRM, also often referred to as multiple reaction monitoring when several precursor-to-product transitions are monitored)<sup>171</sup> and parallel reaction monitoring (PRM) in which selected precursors are specified prior to data acquisition.<sup>172,173</sup> In SRM, the precursors and particular fragment ions originating from the precursors are enumerated to create MS/MS transitions.<sup>171</sup> The targeted SRM method is employed to monitor sets of specific proteins (based on known MS/MS patterns of constituent peptides) in a reproducible and quantitative manner and can typically monitor at most a few thousand peptides per LC run.<sup>171</sup> PRM builds on the same precursor-to-product transition concept as SRM except that all product ions evolving from each specified precursor are detected in parallel at high resolution and accuracy, thus providing a greater number of transitions to confirm peptide identity and alleviating the dependence on preselecting MS/MS transitions.<sup>172,173</sup>

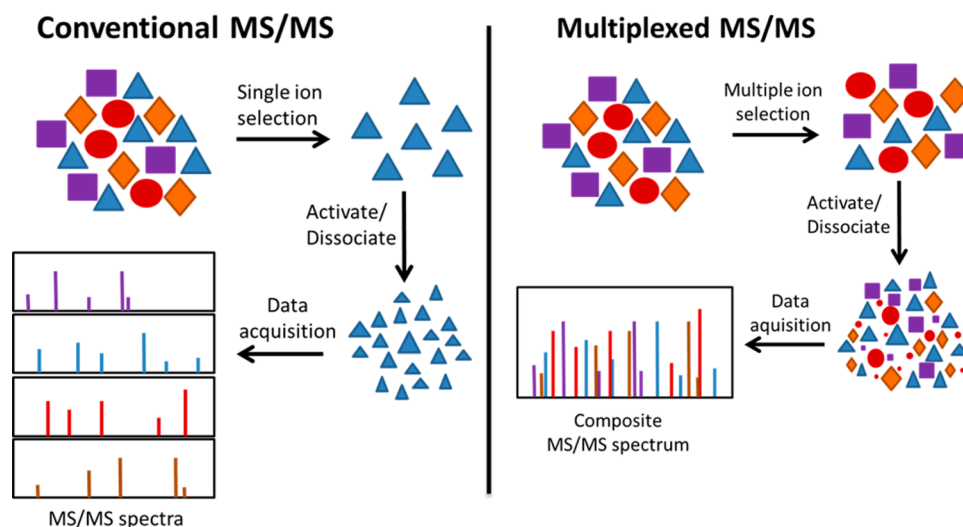


**Figure 3.** Comparison of conventional and multiplex methods for MS/MS data acquisition. Adapted from Multiplexed and data-independent tandem mass spectrometry for global proteome profiling, Chapman, J.D., Goodlett, D.R., Masselon, C.D. *Mass Spectrom. Rev.* **2014**, Vol. 33, 452–470 (ref 168). Copyright 2014 Wiley.

The convention of analyzing peptides in a serial manner by isolation of individual precursors has been widely adopted for automated data collection schemes, especially for targeted applications, but the interest in increasing throughput has motivated the development of other strategies (see Figure 3). Data independent acquisition (DIA) approaches, which are essentially unbiased data collection methods, are based on acquiring MS/MS spectra for sets of precursors that fall within specific windows (for example 25 Da ranges) regardless of ion abundance, thus affording highly multiplexed data collection method.<sup>174–180</sup> These afford measurements of peptides without the specific precursor selection criteria common for SRM and PRM methods, and instead precursor ions are broadly isolated within certain  $m/z$  ranges. The resulting complex fragmentation patterns may be correlated with the time-resolved elution profiles of specific precursor ions, thus allowing identification and profiling of peptides even for coeluting/coisolated species. Measurement of several precursor-to-product transitions facilitates differentiation of true peptides from interferences. Numerous variations of DIA methods have been developed, and their description has been expertly reviewed.<sup>168</sup> In general, numerous benefits have evolved from these data acquisition routines: limited redundancy in collection of MS/MS data, improved confidence in peptide identification and relative quantitation, enhanced detection limits, extended dynamic range and depth of peptide profiling, highly multiplexed data collection, and optimized data acquisition metrics (time, throughput). The overarching impact of this large array of DIA strategies in the context of the present review is that they cleverly showcase the utilization of ion activation/dissociation methods to enhance deeper global proteomics profiling, targeted approaches, and quantitative strategies.

**Utilizing Multiple Activation Methods.** Elaborate comparisons of activation methods via collection of large-scale MS/MS data sets using some combination of HCD, ECD, ETD, and CID in parallel have served several purposes. These comparisons have provided considerable insight into the strengths and shortcomings of individual activation methods and have likewise motivated the strategic use of multiple activation methods to increase the success of peptide identification in high-throughput applications. A number of

benchmark “comparative” studies have been reported over the past decade, most focusing on comparisons and complementary utilization of collisional activation and electron activation methods.<sup>181–194</sup> The ability to effectively exploit the use of multiple activation modes has resulted in the development of elegant algorithms that utilize specific ion metrics (such as charge state) to make on-the-fly decisions about the selection of the activation method. As one of the original landmark examples, a decision-tree method using ETD and CAD methods was developed for analysis of LysC peptides from yeast cell lysates and from human embryonic stem cell lysates that resulted in significantly more peptide identifications than CAD or ETD alone.<sup>182</sup> Using more than one activation method (in alternating scans or separate experimental runs) provides an obvious way to generate more extensive fragmentation information about some of the more intractable molecules, like peptides with post-translational modifications or ones containing disulfide bonds. Spectra obtained from ECD or ETD and CAD have been strategically combined to overcome the limitations of a single activation method.<sup>183–189</sup> In a more recent study, CAD predominantly resulted in cleavages of the glycan portion of glycopeptides, whereas ECD and ETD favored fragmentation of the peptide portion.<sup>193</sup> Using both methods in an alternating manner in which a characteristic neutral loss upon HCD triggered a subsequent ETD step facilitated characterization of O-glycopeptides originating from trypsin digestion of O-glycoproteins from a human cell line.<sup>193</sup> This combined HCD/ETD approach was a promising strategy for targeting glycopeptides and was developed further for analysis of more complex N-linked glycoproteins (ribonuclease B and immunoglobulin G).<sup>190,191</sup> A similar method was developed to streamline the identification of phosphorylation sites of proteins in which a neutral loss of a labile phosphate group upon CID of a peptide triggered subsequent ECD of the same peptide ion.<sup>192</sup>

Combining spectral information obtained using multiple activation modes has been similarly fruitful for expanding the analytical metrics of top-down analysis of intact proteins. In one recent study, CID, IRMPD, ECD, and ETD were used to provide complementary sequence information about RNase B, a glycosylated protein, and its nonglycosylated counterpart

RNase A.<sup>194</sup> Sequence coverage obtained by ETD and ECD was two to three times more extensive than that obtained from CID and IRMPD data, and the glycan was retained which allowed facile assignment of the glycosylation site.<sup>194</sup>

**Hybrid Activation Methods.** In addition to methods that have utilized more than one activation method to expand the depth or breadth of diagnostic fragmentation information, there has been interest in combining activation methods in single experiments to streamline data collection and maximize the benefits of multiple activation modes. This concept was originally successfully employed to improve the fragmentation efficiencies of electron-activation methods (ECD and ETD) for which it was recognized that the large population of charge-reduced precursor ions created by ECD or ETD could be converted into meaningful product ions by additional energization.<sup>60–64</sup> This concept was implemented in several ways, via supplemental activation using IR photons or a heated bath gas or low energy collisions. The use of supplemental activation is now well-established for studies using electron-based methods and is more generally termed activated ion ECD or activated ion ETD.<sup>60–64</sup> Hybrid strategies have extended to other combinations of activation methods that can be engaged simultaneously, including ETcaD, and more recently EThcD<sup>195–198</sup> and ETuvPD,<sup>101,122</sup> and have been demonstrated for both peptides and proteins. In general, ETcaD and EThcD methods are readily implemented on commercial mass spectrometers, thus giving them versatility for many applications. ETcaD was one of the original hybrid concepts, in which low energy collisional activation was used to specifically excite the prevalent charge-reduced precursor ions produced during the electron-transfer process (essentially the ETnoD dead-end).<sup>64</sup> The ETcaD method significantly improved the fragmentation efficiency and led to higher abundances and more extensive arrays of the c- and z-ions commonly generated by ETD.<sup>64</sup> In EThcD, ETD is followed by HCD of all products created upon electron transfer activation, including both the charged-reduced and unreacted “surviving” precursor ions.<sup>195–198</sup> EThcD resulted in production of a combination of c/z and b/y fragment ions that afford richer MS/MS spectra. One example illustrating a comparison of ETD, ETcaD, HCD, and EThcD spectra for peptide EGVNDNEEGFFSAR is shown in Figure 4.<sup>195</sup> Individually, the ETD and HCD spectra display fewer diagnostic sequence ions. The EThcD spectrum exhibits a blend of both HCD and ETD fragment ions and results in very higher sequence coverage.<sup>195</sup>

The most extensive studies of hybrid activation methods have typically been undertaken in conjunction with systematic comparisons to conventional single-mode activation techniques, both for peptides and for intact proteins.<sup>195–198</sup> EThcD for peptides resulted in a greater degree of backbone fragmentation and higher confidence in pinpointing sites of modifications. Although the total number of peptides identified based on EThcD mass spectra was comparable or slightly lower than the number identified by HCD alone (and significantly higher than ETD alone), the sequence coverage obtained for the peptides was notably greater. For phosphopeptides, the sites of phosphorylation were identified with greater confidence, in large part because of the production of dual series of fragment ions (b/y and c/z).<sup>196</sup> The EThcD method was also applied for the identification of disulfide bonds in proteins based on the cleavage of S–S bonds by ETD for peptides produced from pepsin digestion.<sup>197</sup> HCD was used to increase the formation of backbone fragment ions. The effectiveness of

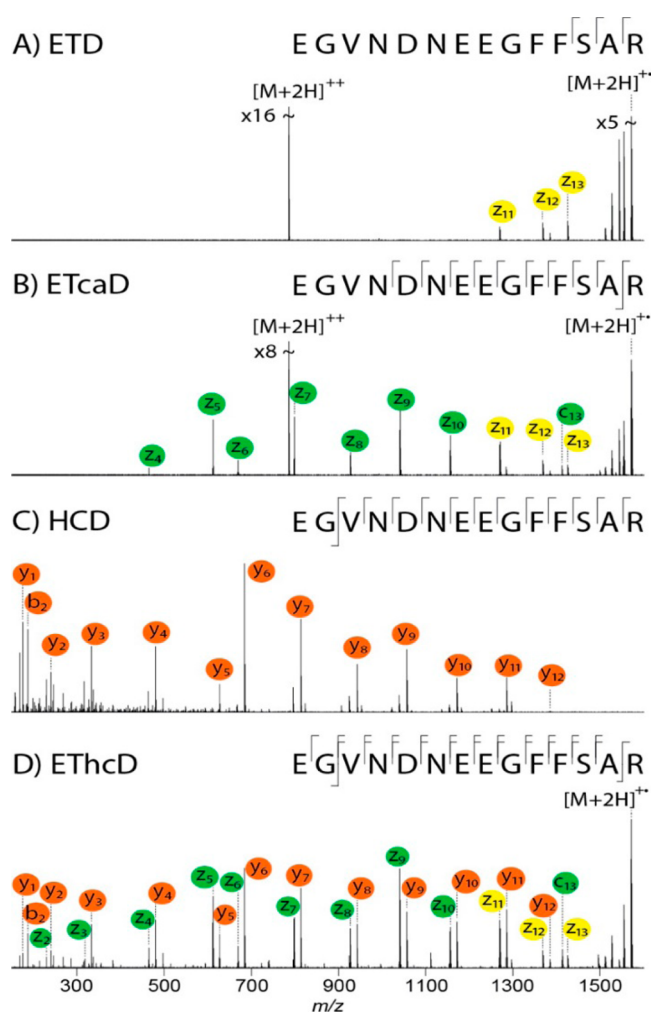


**Figure 4.** Examples of peptide fragmentation by (A) ETD, (B) ETcaD, (C) HCD, and (D) EThcD for peptide EGVNDNEEGFFSAR. Reproduced from Frese, C.K., Altelaar, A.F.M., van den Toorn, H., Nolting, D., Griep-Raming, J., Heck, A.J.R., Mohammed, S. *Anal. Chem.*, **2012**, *84*, 9668–9673 (ref 195). Copyright 2012 American Chemical Society.

the method was demonstrated for identification of disulfide bonds in therapeutic antibodies.<sup>197</sup> The EThcD strategy was applied for the high-throughput analysis of human leukocyte antigen peptides, resulting in identification of over 12 000 peptides from a human B-cell line and affording a significantly higher success rate of peptide identification compared to HCD or ETD alone.<sup>198</sup>

Electron-based activation has also been combined with UVPD,<sup>101,122</sup> in which hydrogen-rich peptide ions (essentially radical peptide ions created from ETnoD) or proteins were subjected to UVPD. For simple peptides containing a single Arg at the terminus, production of a-type ions was favored when the Arg was located at the N-terminus, whereas c/z ions dominated when the Arg was positioned at the C-terminus.<sup>101</sup> This Arg-specific outcome was attributed to whether the peptides adopted elongated helices (C-terminal Arg) or more compact globular conformations (N-terminal Arg). The ability to map new phosphorylation sites using the hybrid ET-UVPD method was demonstrated for the kinase domain of TRPM7/ChaK1.<sup>101</sup> In another study, ETuvPD resulted in formation of a greater array of complementary fragment ion pairs for analysis of intact proteins.<sup>122</sup> This method offered the ability to

modulate the distribution of a/x and c/z ions that are typically formed by UVPD and ETD, respectively, as well as reduce spectral congestion by increasing the distribution of fragment ions across a greater  $m/z$  range.<sup>122</sup>

**Separations.** The coupling of tandem mass spectrometers to a variety of innovative separation methods has led to enormous gains in the number, depth, and breadth of peptides identified based on their MS/MS spectra.<sup>24</sup> An exhaustive and/or inclusive summary of high impact LC–MS/MS studies is prohibitive, but several are cited herein to show examples of the significant gains in the field of high-throughput peptide-based and protein-based proteomics.<sup>199–203</sup> The majority of studies have used collisional activation methods (CID, HCD) for peptide identification, again showcasing the vital role that ion activation has played in these impressive high-throughput MS/MS-based proteomic studies. For example, a strategy using ultralong, shallow gradients was used to identify over 2700 proteins (via ~18 000 peptides) from a HeLa cell lysate based on CID mass spectra.<sup>199</sup> Monolithic silica-C18 capillary columns were employed for separation and CID of tryptic peptides from pluripotent stem cells, resulting in identification of nearly 100 000 peptides representing 9500 proteins.<sup>200</sup> Deep phosphopeptide profiling was accomplished using a strategy that coupled phosphopeptide enrichment with nanoLC–MS/MS.<sup>202</sup> This method resulted in identification of nearly 8 000 phosphoproteins based on 50 000 phosphopeptides from HeLa S3 cells.<sup>202</sup> In another study over 34 000 peptides, corresponding to nearly 4 000 proteins per hour of run time, were identified in a high-throughput analysis of the yeast proteome.<sup>203</sup> Capillary electrophoresis has gained ground as an alternative separation method to nanoscale liquid chromatography for proteolytic digests.<sup>204,205</sup> For example, over 10 000 peptides accounting for 2 000 proteins were identified from a 100 min analysis of a HeLa cell digest using capillary zone electrophoresis with CID as the ion activation method.<sup>204</sup> Along those same lines, CZE–MS/MS (based on CID) was used to identify over 2 000 phosphopeptides from an MCF-10A cell line.<sup>205</sup>

These are just a few examples demonstrating the utilization of CID data for high-throughput identification of peptides. Other high-throughput studies have used ETD, IRMPD, or UVPD or combinations of MS/MS methods.<sup>85,112,206,207</sup> As examples of large-scale LC–MS studies using ETD, thousands of peptides were identified from Lys-C digestion of the proteins from stem cell lysates,<sup>206</sup> and a study of large secretory peptides ranging up to 15 kDa was reported using CID and ETD in alternating LC runs to expand the number of peptides identified and improve localization of phosphorylation sites.<sup>207</sup> The use of IRMPD for a large-scale LC–MS/MS study of the yeast proteome was presented, identifying thousands of tryptic peptides and finding that IRMPD matched or slightly out-performed conventional low-energy CID for the same samples.<sup>85</sup> In addition, the use of IRMPD allowed formation and detection of low mass tandem mass tag (TMT) reporter ions which facilitated quantitative profiling.<sup>85</sup> In an application that used UVPD as the ion activation method, 3663 peptides, corresponding to 805 proteins, were identified from *Halobacterium salinarum* lysates, and 2350 peptides, corresponding to 659 proteins, were identified from HeLa tryptic lysates.<sup>112</sup>

## ■ TOP-DOWN AND MIDDLE-DOWN METHODS

There have been an enormous number of studies used to identify or characterize proteins based on the bottom-up approach which relies on the fragmentation patterns of peptides to identify proteins. As noted above, many activation methods (CID, HCD, ECD, ETD, IRMPD, UVPD) have been utilized very effectively in the bottom-up approaches. The general bottom-up workflow has been extremely popular because smaller molecules (i.e., peptides) are more successfully separated, ionized, and fragmented than larger molecules (i.e., proteins). The alternative top-down and middle-down strategies for protein identification have gained momentum in recent years.<sup>19–23,208,209</sup> The increasing scope of top-down and middle-down studies is related, in part, to improvements in ion activation methodologies that have allowed more extensive fragmentation of intact proteins (top-down) or large polypeptides (middle-down). At the same time, high-performance mass analyzers have facilitated high-accuracy/high-resolution measurements of extremely complex and congested mass spectra of very large ions, and powerful algorithms have allowed assignment of the fragment ions and identification of the proteins. Advances in top-down methods have been showcased in a number of review articles,<sup>19–23,208,209</sup> and thus only a handful of key studies in the most recent few years are highlighted here to demonstrate the range of ion activation methods that have been utilized for very impressive outcomes.

Similar to the manner that trends in peptide fragmentation pathways have been analyzed in detail as noted earlier, a number of studies have examined trends in the fragmentation channels of proteins for different activation methods, particularly as a function of protein charge state. Upon collisional activation, proteins in higher charge states tend to fragment more readily (i.e., using less energetic activation conditions) than lower charge states, a trend also noted for peptides.<sup>210,211</sup> This correlation is attributed to the proton mobility effect, in which amide bond cleavage is modulated by intramolecular proton mobilization.<sup>46,47</sup> Another outcome for proteins that is analogous to collisional activation of peptides is the preferential backbone cleavage next to proline (for higher charge states) and conversely cleavages after aspartic and glutamic acids as well as loss of ammonia and water for lower charge states.<sup>210,211</sup> Proteins in intermediate charge states tend to give the greatest variety of amide bond cleavages (formation of b/y ions), a result that reflects substantial proton mobility and minimization of highly preferential cleavages. Moreover, proteins in intermediate charge states undergo more extensive internal cleavages, a feature not observed for peptides, as well as significant fragmentation C-terminal to Pro and Asn and N-terminal to Ile, Leu, and Ser.<sup>210,211</sup> It was surmised that the protons associated with proteins in low charges were more strongly localized at highly basic sites and additionally solvated by auxiliary intramolecular interactions.<sup>210</sup> In contrast, highly protonated proteins were predicted to be more elongated and experience greater Coulombic effects. Extension of collisional activation methods to high throughput large-scale top-down proteomics studies have, in fact, been somewhat impeded by the dominance of some of these strong preferential backbone cleavages at the most labile bonds, including Xxx-Pro, Asp-Xxx, and Glu-Xxx.

The use of ETD was evaluated in detail for characterization of proteins in the range of 30–80 kDa.<sup>212</sup> Overall sequence coverage decreased with the mass of the protein from the

confounding factors of decreasing sensitivity, interfering effects of charge-reduced ions, and production of unassigned or overlapping internal ions. Both CAD and ECD were used in a complementary fashion on an FTICR mass spectrometer to characterize a 55 kDa amylase protein from saliva, in particular focusing on the ability to pinpoint five disulfide linkages of the protein.<sup>213</sup> Just as auxiliary activation improved the analytical metrics of peptide fragmentation based on electron-activation methods, supplementary activation also enhanced the performance of ETD for analysis of intact proteins.<sup>68</sup> AI-ETD was utilized for characterization of intact proteins up to 29 kDa. In this study, infrared photoirradiation was used to increase the disassembly of fragment ions that remained held together by various noncovalent interactions after ETD of proteins.<sup>68</sup> In the context of quantitative metrics such as the number of matched fragment ions for different charge states of proteins, AI-ETD outperformed HCD and afforded higher protein sequence coverage than HCD or ETD.<sup>68</sup>

The performance metrics of different activation methods have been compared and combined to provide more comprehensive sequence coverage of proteins, especially those containing PTMs for which localization of modifications is essential. For example, HCD and ETD were used for characterization of an N-terminal segment from the phosphoprotein Protein aurora borealis, and it was found that the hybrid methods ETcId and EThcD afforded more extensive sequence coverage than ETD alone.<sup>214</sup> The deeper coverage facilitated pinpointing the phosphorylation sites of the 17.5 kDa protein.<sup>214</sup> Another study reported the identification of over 150 integral membrane proteins from human H1299 cells based on ETD, low-energy CAD, and HCD.<sup>215</sup> Interestingly, ETD resulted in cleavages predominantly in the soluble regions, whereas the two collisional activation methods favored cleavages in transmembrane domains for which fragmentation was modulated heavily by proton mobility.

Owing to the fact that antibodies are among the largest proteins and because therapeutic monoclonal antibodies are one of the fastest growing sectors of the pharmaceutical market, the characterization of these ~150 kDa molecules is a particularly daunting challenge. Both top-down and middle-down methods have been used to characterize antibodies, their variants, and impurities during production. Up to 33% sequence coverage of a Humira IgG1 was obtained by top-down characterization of the intact protein using ETD.<sup>216</sup> The same group also used an alternative middle-down strategy that used IdeS protease (an immunoglobulin G-degrading enzyme of *Streptococcus pyogenes*)<sup>217</sup> to cleave antibodies at the hinge region, reduction of disulfide bonds to produce light and heavy chain fragments around 25 kDa in size, followed by ETD of the subunits.<sup>218</sup> Characterization of the resulting large antibody fragments using ETD resulted in up to 68% sequence coverage by combining MS/MS data from multiple runs using varying electron activation times.<sup>218</sup> A middle-down approach was used to examine impurities and variants of monoclonal antibodies based on HCD of the heavy and light chains, obtaining sequence coverages in the range of up to 46% for the light chains and 20% for the heavy chains.<sup>219</sup> In another study, the fragment ion information from both ECD and ETD activation methods and from both top-down and middle-down approaches was combined to analyze several IgG fusion proteins, ultimately obtaining sequence coverage of 61%.<sup>220</sup>

Significant inroads in the application of top-down strategies for high-throughput top-down proteomics have also been

reported. One study identified over 1650 proteoforms, corresponding to 563 proteins, from *Salmonella typhimurium* during a 4 h elution.<sup>221</sup> In the one of the most extensive large-scale top-down study to date a four dimensional separation strategy with 12 T FTICR-MS was used to identify over 1 000 gene products representing over 3 000 proteoforms from human HeLa S3 cells.<sup>222</sup> Many of the proteoforms contained phosphorylations, acetylations, and methylations.<sup>222</sup> The separation strategy needed to accomplish this feat incorporated solution isoelectric focusing, electrophoresis (gel-eluted liquid fraction entrapment electrophoresis GELFrEE based on protein size and isoelectric point), and nanoscale liquid chromatography.<sup>222</sup> Proteins over 100 kDa were successfully identified based on high-accuracy mass measurements and MS/MS via ETD, HCD, or CID. This impressive study was eclipsed by an even larger study reported in 2013 in which over 1200 proteins were identified from a transformed H1299 human cell line, corresponding to over 5 000 proteoforms and including nearly 350 mitochondrial proteins.<sup>223</sup> For this study, a data dependent MS/MS strategy using CID, HCD, and ETD was enabled.<sup>223</sup>

Although the large majority of high-throughput top-down proteomics analyses have utilized conventional nanoscale reversed phase liquid chromatographic separations, two emerging methods have shown promise for expanding the portfolio of methods suitable for proteins. These alternative methods, capillary electrophoresis (CE) and ion mobility, provide separation based on mass-to-charge or molecular structure, respectively, rather than hydrophobicity. In comparison to liquid chromatographic methods, capillary electrophoresis methods offer the merits of low sample consumption, high efficiency, and speed. In a study that coupled capillary zone electrophoresis for separation and HCD for characterization of intact proteins, four proteins up 66 kDa in size were identified, although the total sequence coverage obtained for each protein was relatively low.<sup>224</sup> CZE was integrated with AI-ETD for analysis of proteins from a *Mycobacterium marinum* bacterial secretome, resulting in identification of 41 proteoforms.<sup>225</sup> Another study identified 30 proteins ranging from 30 to 80 kDa using capillary electrophoresis with HCD as the ion activation method for protein characterization.<sup>226</sup> One top-down CE-MS study analyzed *Pyrococcus furiosus* using HCD and CID in a data-dependent manner during a sub-30 min run, leading to identification of up to 144 proteoforms per fraction and a total of 291 proteoforms for three runs.<sup>227</sup> Ion mobility has also provided another innovative opportunity to increase the dynamic range and resolution of top-down analysis. One recent study reported the integration of ion mobility with a high-performance mass spectrometer for analysis of intact proteins. Ion mobility was used as a means to disperse the fragment ions produced upon CID of proteins, thus alleviating congestion from overlapping fragment ions.<sup>228</sup>

In light of the growing interest in and payoffs of top-down MS/MS methods for characterization of proteins, it is well-recognized that a large fraction of the hundreds of fragment ions produced upon activation of proteins or large peptides are not identified. This gap primarily arises from the fact that database search algorithms developed for protein fragmentation focus on N-terminal and C-terminal ions, not internal ions which contain neither terminus. As such, an effort to account for internal ions in top-down proteomics was undertaken as a means to increase confidence in identification and characterization of proteoforms.<sup>229</sup> The report detailed the formation and assignment of internal ions using ubiquitin in several

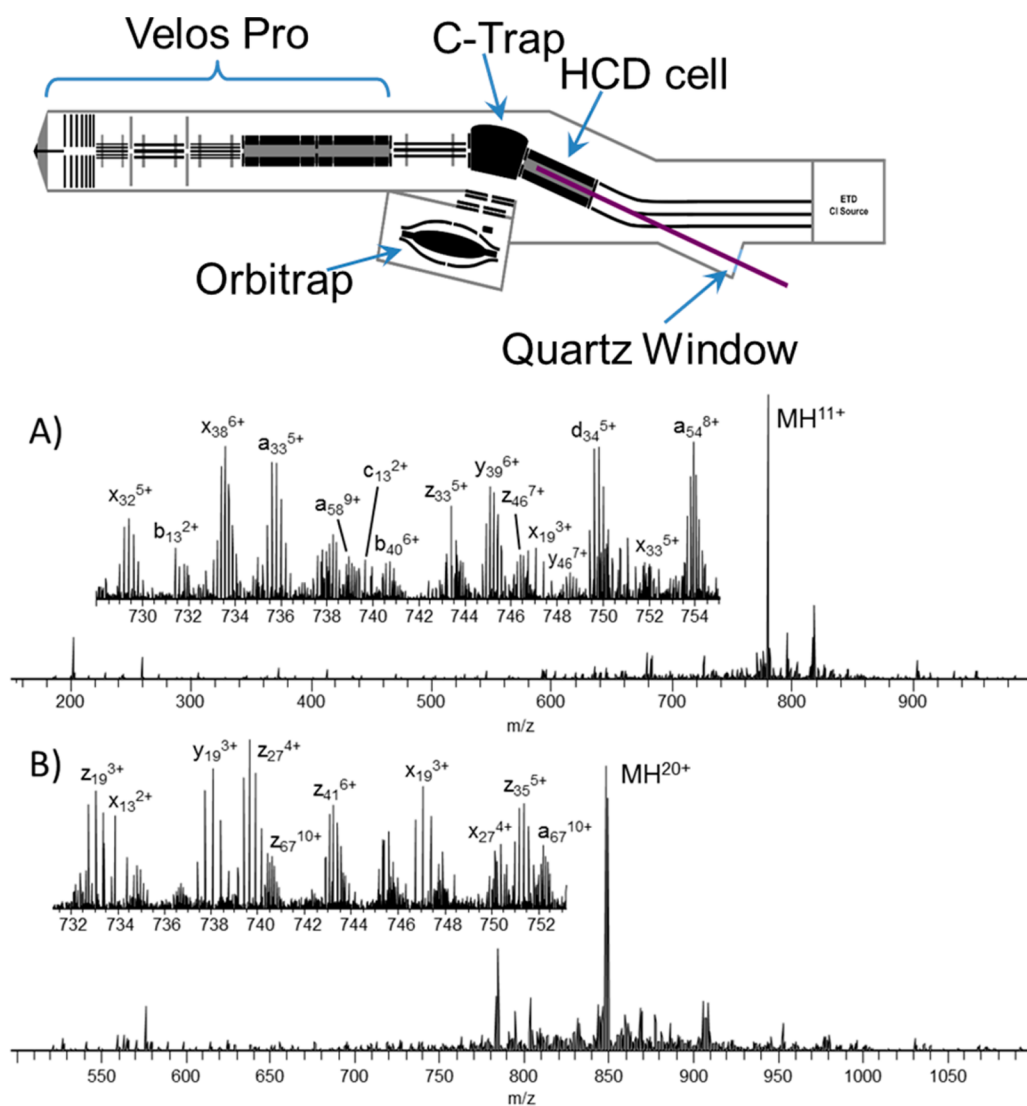


**Figure 5.** Schematic of Orbitrap mass spectrometer equipped with laser for photodissociation and examples of UVPD mass spectra of the (A) 11+ charge state of ubiquitin and (B) the 20+ charge state of myoglobin. Reproduced from Shaw, J.B., Li, W., Holden, D.D., Zhang, Y., Griep-Raming, J., Fellers, R.T., Early, B.P., Thomas, P.M., Kelleher, N.L., Brodbelt, J.S. *J. Am. Chem. Soc.* **2013**, *135*, 12646–12651 (ref 116). Copyright 2013 American Chemical Society.

charge states as a test-bed case. In particular, the energy required for formation of internal ions was similar to the amount need for production of conventional N- and C-terminal ions (b/y).<sup>229</sup> Deciphering internal ions should increase sequence coverage metrics and aide in localization of PTMs, thus motivating the ongoing interest in developing more sophisticated algorithms to support assignment of internal ions.

In contrast to the more well-established collisional and electron-based activation methods, UVPD is the newest activation method applied for characterization of intact proteins.<sup>116–122</sup> UVPD using 193 nm photons was implemented on a high-performance Orbitrap mass spectrometer to allow high-accuracy/high-resolution measurements of the rich array of fragment ions produced upon photoactivation of proteins.<sup>116</sup> A schematic of the modified mass spectrometer is shown in Figure 5, along with representative UVPD mass spectra for two proteins (ubiquitin (11+) and myoglobin (20+)). A single 5 ns laser pulse was used to activate protein ions stored in the HCD cell prior to transfer of the product ions to the Orbitrap analyzer for analysis.<sup>116</sup> The predominant types

of ions generated by UVPD were a, x, y, and z ions with fewer and lower abundances of b, c, v, w, and d ions. With respect to sequence coverages, UVPD outperformed HCD, CID, and ETD and showed relatively low dependence on protein charge state in contrast to the other activation methods for which sequence coverage decreased as a function of charge state (HCD, CID) or increased with charge state (ETD).<sup>116</sup> The high sequence coverage (in terms of the number of interresidue cleavages along the backbone) of UVPD made it a natural fit for mapping PTMs and incorporation of unnatural amino acids into proteins. This attribute of UVPD was demonstrated for the identification of oxidation sites (such as shown for peptidyl-prolyl cis/trans isomerase Pin1) and point mutations in sequence variants.<sup>116</sup> In another study, 193 nm UVPD was used to examine variants of green fluorescent protein (GFP) with molecular weights in the range of 28 kDa.<sup>119</sup> UVPD afforded a larger number of informative sequence ions originating from backbone cleavages, ultimately allowing confident localization of sites of mutagenesis in which basic amino acids replaced the canonical residues.<sup>119</sup> UVPD also

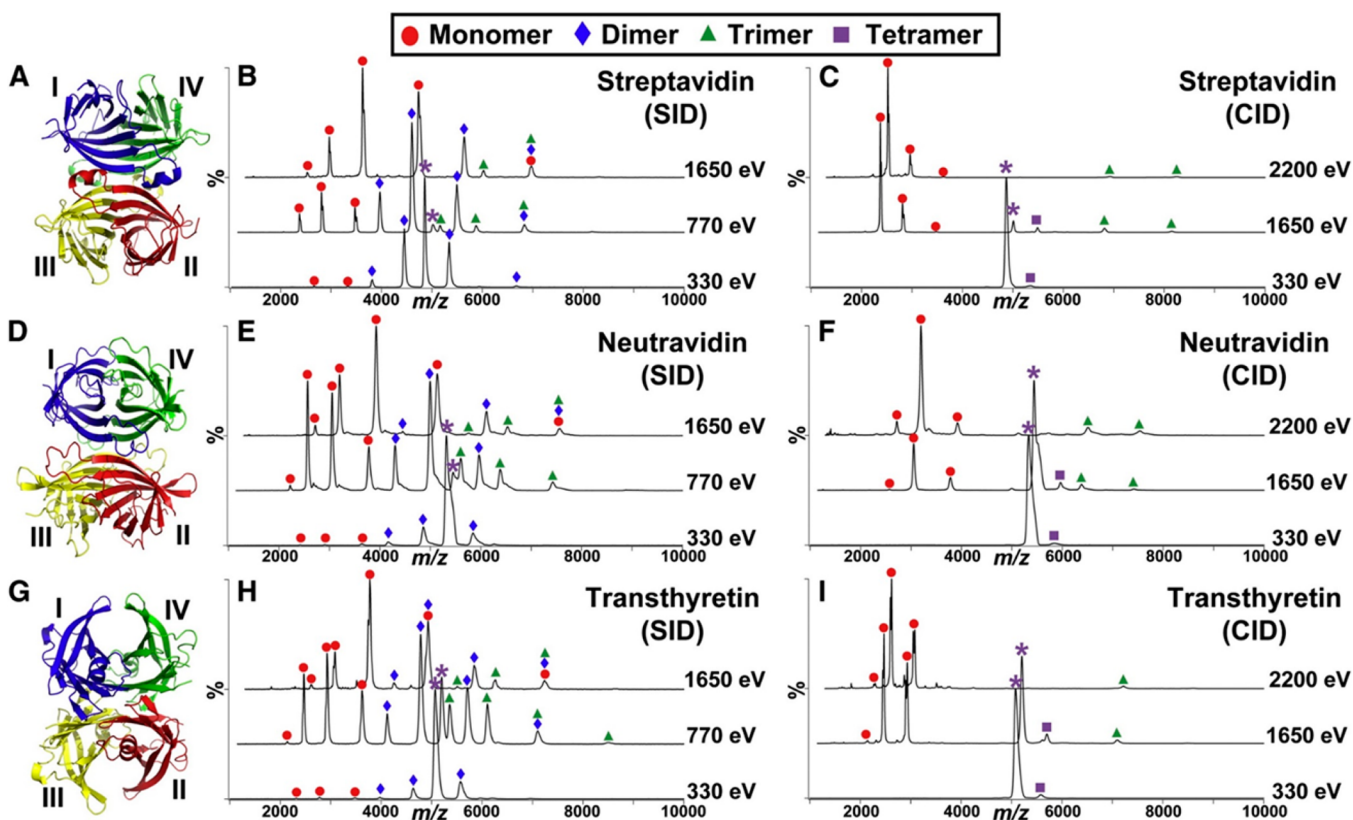


**Figure 6.** Nanoelectrospray SID (middle panel) and CID (right panel) mass spectra of the charge-reduced 11+ precursor of (B and C) streptavidin (SA), (E and F) neutravidin, and (H and I) transthyretin (TTR) at three separate collision energies. All fragments are labeled based on their corresponding peaks detected in ion mobility (IM). The precursor ion in each spectrum is indicated by a purple asterisk. Crystal structures of (A) SA (PDB 1SWB), (D) neutravidin (PDB 1VYO), and (G) TTR (PDB 1F41) are shown in the left panel. Subunits I, II, III, and IV are also shown in blue, green, yellow, and red, respectively. Reproduced from *Chemistry & Biology*, Vol. 22, Quintyn, Q., Yan, J., Wysocki, V.H., Surface-Induced Dissociation of Homotetramers with D2 Symmetry Yields their Assembly Pathways and Characterizes the Effect of Ligand Binding, pp. 583–592, Copyright (2015), (ref 142) with permission from Elsevier.

demonstrated fragmentation deeper into the interior (mid-section) of the protein sequence.<sup>119</sup> These attributes of UVPD also proved useful for locating individual unnatural amino acids incorporated into proteins created via compartmentalized partnered replication, an innovative molecular engineering method.<sup>117,120</sup> For example, the fragmentation patterns created by UVPD allowed the identification of 5-hydroxyl-L-tryptophan in place of tryptophan<sup>117</sup> and selenocysteine instead of cysteine<sup>120</sup> in dihydrofolate reductase (a 19 kDa protein).

To demonstrate the capabilities of UVPD for high-throughput top-down proteomics, an LC–MS strategy was reported for characterization of ribosomal proteins from *E. coli* as well as fractions of a *S. cerevisiae* (yeast) lysate.<sup>118</sup> On the basis of UVPD, 46 ribosomal proteins were identified compared to 44 using HCD, virtually all with high sequence coverages from the greater numbers of matched fragment ions. For the *S. cerevisiae* lysate, 292 distinct proteoforms were identified corresponding to 215 different proteins, of which 168 contained some type of post-translational modification.<sup>118</sup>

As the name implies, middle-down approaches are an intermediate between top-down (analysis of intact proteins) and bottom-up (peptide-based analysis) strategies. For middle-down analysis, proteins are subjected to limited proteolysis or are digested using highly selective proteases that typically result in large peptides in the range of 3–25 kDa. The growing recognition that middle-down methods may offer an attractive alternative to top-down and bottom-up approaches has spurred

new interest, and there has been significant application of middle-down methods for analysis of histones,<sup>230–236</sup> as well as for characterization of ubiquitination.<sup>237,238</sup> In one of the most recent studies, bottom-up (using HCD) and middle-down (based on ETD) approaches were compared for determination of relative abundances and stoichiometries of PTMs of histone H3, and it was found that both activation methods returned similar results and allowed extensive mapping of modifications.<sup>235</sup>

## ■ NATIVE PROTEINS AND PROTEIN COMPLEXES

The development of new mass spectrometry methods has opened many new avenues for exploring aspects of structural biology. The ability to investigate structures of proteins, protein–ligand complexes, and macromolecular complexes in the gas phase is facilitated by the use of native-spray methods to transfer native-like proteins and complexes into the gas phase. Proteins are sprayed from buffered solutions to preserve noncovalent interactions, thus allowing subsequent high mass analysis, ion mobility measurements, and MS/MS strategies to interrogate the structures.<sup>239–242</sup> Complexes as large as 18 MDa have been transferred to the gas phase using native-spray conditions.<sup>243</sup> Analysis of such large macromolecules present substantial hurdles, especially in the context of identifying the individual protein subunits, unravelling how the individual protein constituents are assembled, and deciphering conformational changes that occur during assembly of protein complexes

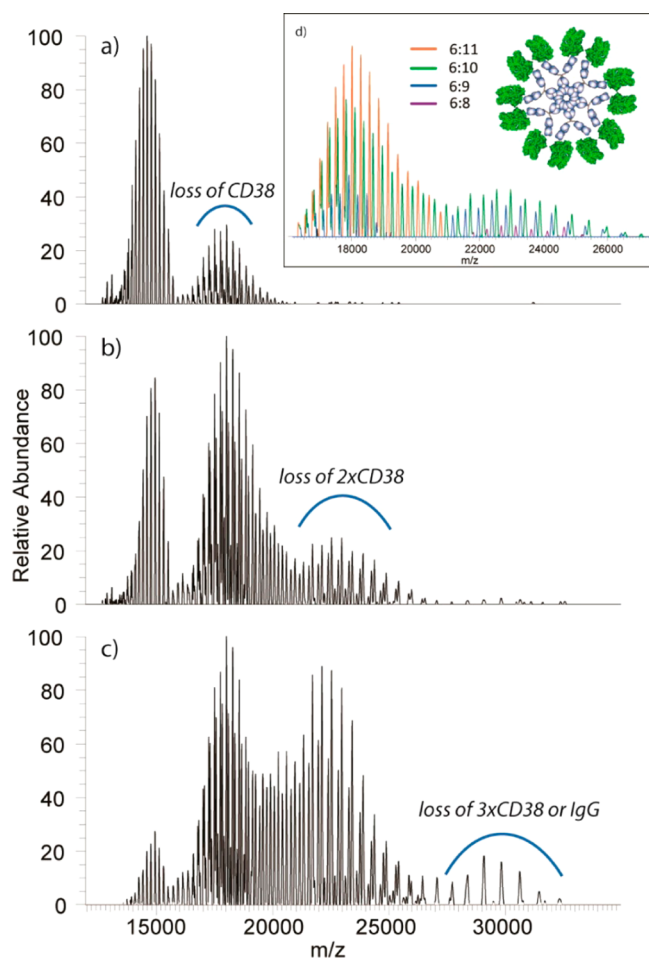


**Figure 7.** Broadband isolation of the antibody hexamer in complex with CD38 antigen molecules followed by collisional dissociation at acceleration voltages of (a) 100 V, (b) 150 V, and (c) 200 V. (d) Color annotation of fragment ions produced by collisional dissociation of the IgG1-005 hexamer:CD38 complex at 150 V colored according to the number of CD38 subunits present; the inset schematically shows suggested spatial arrangement of the subunits in the complex. As the dominant fragment ions series corresponds to an IgG:CD38 complex of 6:11, the predominant precursor ions should have been the 6:12 IgG:CD38 complex. Reproduced from Dyachenko, A., Wang, G., Belov, M., Makarov, A., de Jong, R.N., van den Bremer, E.T., Pareren, P.W.H.I., Heck, A.J.R. *Anal. Chem.* **2015**, *87*, 6095–6102 (ref 264). Copyright 2015 American Chemical Society.

or protein–ligand complexes. All of these challenges have been addressed by a number of innovative ion activation strategies.<sup>10–28</sup>

Low-energy collisional activation of macromolecular complexes typically results in disruption of noncovalent interactions, leading to disassembly of the protein constituents.<sup>244</sup> Low-energy collisional activation provides insight into the subunit composition of the complexes (stoichiometry) but not sequence information about the individual proteins.<sup>244</sup> Other ion activation methods, including higher kinetic energy beam type CID<sup>245</sup> and higher energy collisional dissociation (HCD),<sup>246,247</sup> surface induced dissociation (SID),<sup>138–144</sup> electron capture dissociation (ECD),<sup>248–254</sup> electron transfer dissociation (ETD),<sup>255–257</sup> and photodissociation,<sup>258–263</sup> have also been used to evaluate structures of native proteins and protein complexes.

For characterization of macromolecule interfaces, surface induced dissociation (SID) utilizes high energy collisions between macromolecular ions and a surface.<sup>137,139</sup> SID causes disassembly of macromolecular complexes prior to unfolding of the individual proteins, an ideal outcome for mapping contacts between protein subunits.<sup>138–144</sup> This method has provided an exceptional means to reconstruct the quaternary structures of protein complexes, as initially demonstrated for transthyretin tetramers and serum amyloid P decamers,<sup>137</sup> then subsequently reported for complexes comprised of tetradecameric GroEL,<sup>138</sup> dimeric phosphorylase B,<sup>140</sup> and hexameric glutamate dehydrogenase,<sup>140</sup> as well as a multiunit ribonucleoprotein complex.<sup>141</sup> Examples of the SID and CID mass spectra obtained for tetrameric complexes of streptavidin, neutravidin, and transthyretin are shown in Figure 6.<sup>142</sup> The SID spectra at various collision energies reveal that these tetrameric proteins dissociate to yield monomeric and trimeric species as well as dimeric ions not observed upon CID.<sup>142</sup> The formation of dimeric products suggest that some portion of the tetrameric complexes exist as dimers of dimers, as evidence by the release of dimeric subunits upon disassembly of the tetramers.<sup>142</sup> In contrast, CID results in production of monomers and trimers, indicative of unfolding and release of a monomer.<sup>142</sup> In essence, SID of various multimeric protein complexes led to formation of subunits (such as dimers, trimers, tetramers, etc.) that revealed the subunit packing features. In contrast, collisional activation of the same types of complexes primarily led to unfolding of the constituent proteins and disassembly by indiscriminate release of monomers.<sup>142</sup> SID has proven to be a very innovative approach for providing insight into topologies of native protein complexes, especially with respect to the interfaces of the complexes.

Electron capture dissociation (ECD) has been the most popular activation method to date for analysis of intact proteins (as described earlier) and has also been successfully applied for characterization of macromolecular protein assemblies.<sup>248–254</sup> ECD produces extensive series of *c/z*-type sequence ions of proteins. At the same time, some noncovalent interactions survive the electron capture activation process, allowing the ability to map protein–ligand contacts.<sup>248–254</sup> The propensity of ECD for cleavage of backbone bonds that occur in the more flexible regions of proteins or complexes has been used to support a correlation between ECD efficiency and *B*-factors of proteins (where *B*-factors define the degree of flexibility or rigidity of a protein).<sup>251–255</sup> Using a hybrid ion-mobility time-of-flight mass spectrometer, the most flexible regions of alcohol dehydrogenase were mapped by tabulating the relative abundances of diagnostic *c* and *z* ions.<sup>255</sup> For the largest complex studied by ECD, ECD was used to characterize a 158 kDa protein complex consisting of a tetramer of aldolase, resulting in sequencing of 168 residues at the C-terminal end among 463 total amino acids.<sup>248</sup> It was determined that the dominant backbone cleavages occurred in the flexible regions and surface regions of the protein. As noted earlier, electron-based methods in general are less effective for ions in low charge states, and this factor is more prominent for native-like proteins which adopt low charge states (representative of compact, folded native-like structures) upon naturespray.

HCD was used to analyze the native form of the therapeutic antibody-drug conjugate (ADC) bentruximab vedotin, and the fragmentation patterns confirmed that the drug was conjugated to cysteine residues located in both the heavy and light chains.<sup>264</sup> For this study, a multiplexing method was employed

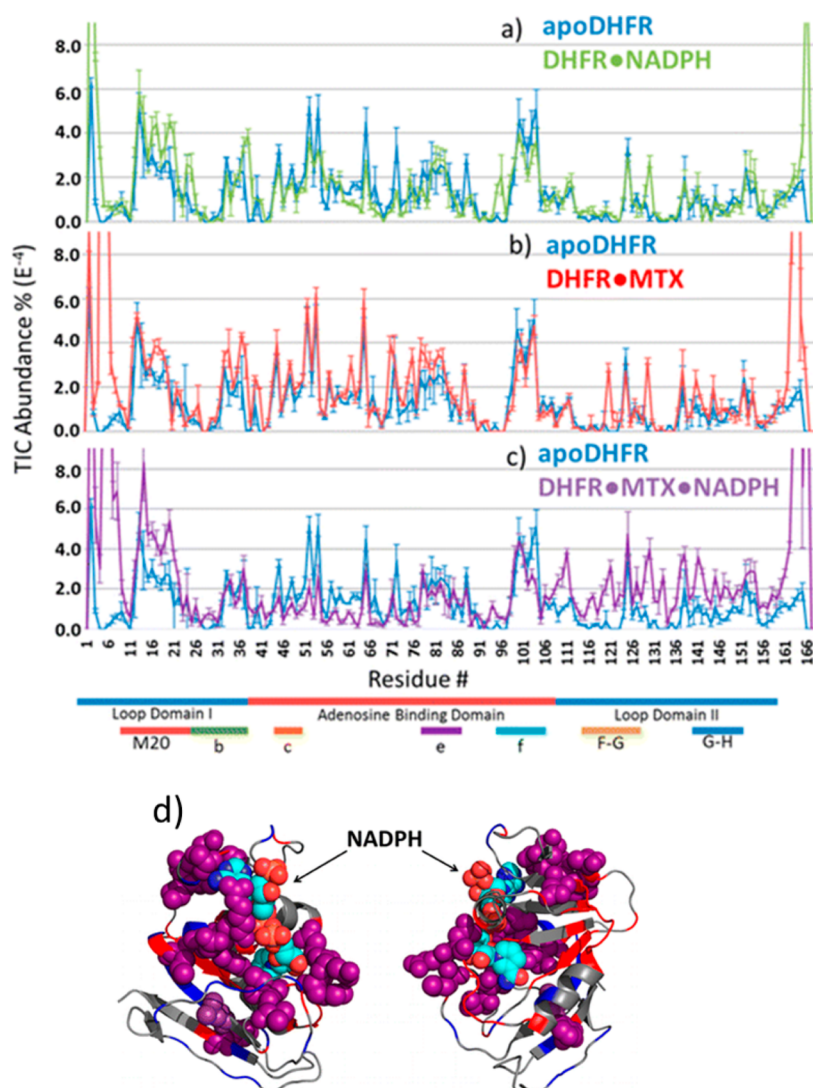


**Figure 8.** Plots of TIC abundance per residue based on summed holo + apo product ions (including both N-termini and C-termini ions) from DHFR and its respective complexes DHFR-NADPH (a), DHFR-MTX (b), and DHFR-NADPH-MTX (c). The 9+ charge state was selected for all experiments. The color code used for each protein is shown in the legends. Standard deviations were calculated from four replicates. (d) Space-filled model of NADPH (in blue/red/orange spheres) and the predicted interacting residues of DHFR (purple spheres) based on UVPD fragmentation. The residues of DHFR presumed to interact with NADPH correspond to those that show overlapping N- and C-termini holo ions from backbone cleavages upon UVPD. Other holo (NADPH-containing) fragment ions from the N-terminus are highlighted in blue, and other holo (NADPH-containing) fragment ions from the C-terminus are highlighted in red (nonspace filled). Reproduced from Cammarata, M.; Thyer, R.; Rosenberg, J.; Ellington, A.; Brodbelt, J.S. *J. Am. Chem. Soc.* **2015**, *137* (28), 9128–9135 (ref 263). Copyright 2015 American Chemical Society.

to sequentially isolate and activate different charge states of the ADC, ultimately allowing efficient dissociation and sufficient signal-to-noise to yield high-quality HCD spectra.<sup>264</sup> Via an elegant combination of experiments involving analysis of ADCs containing different number of drugs, in some cases combined with reduction using dithiothreitol to cleave interchain disulfide linkages, high-resolution maps of the ADCs, including the locations of the drugs, were developed. Moreover, HCD of hexameric complexes associated with CD38 antigen molecules provided insight into the arrangement of the subunits in the enormous assemblies (>1 MDa molecular weight)<sup>264</sup> (see Figure 7). A broad population of IgG1:CD38 assemblies containing six immunoglobulins (IgG) and up to 12 CD38 antigens were isolated and subjected to HCD. As the accelerating voltage (for HCD) was increased, loss of two or three antigens occurred as well as up to one antibody molecule.<sup>264</sup> This strategy combined collisional activation

with high mass analysis to provide insight into the stoichiometry of antigen binding and spatial arrangement of the constituent proteins.

Vacuum UVPD was used to analyze a small protein (IB5)/tannin complex based on 16 eV synchrotron radiation.<sup>258</sup> By mapping those product ions that retained the tannin ligand, the binding site of the IB5 protein was elucidated. UVPD was also integrated with ion mobility to examine the fragmentation of different conformers of ubiquitin.<sup>259</sup> Unique fragment ions that revealed conformer-specific signatures were identified in the UVPD mass spectra. Moreover, cis/trans isomerization of a proline peptide bond resulted in changes in the efficiency of UVPD fragmentation (based on variations in fragment ion abundances).<sup>259</sup> UVPD (193 nm) has been used to characterize the sequences and structures of native proteins and protein–ligand complexes, as well as map the binding sites of the ligands.<sup>260–263</sup> Variations in the efficiencies of backbone

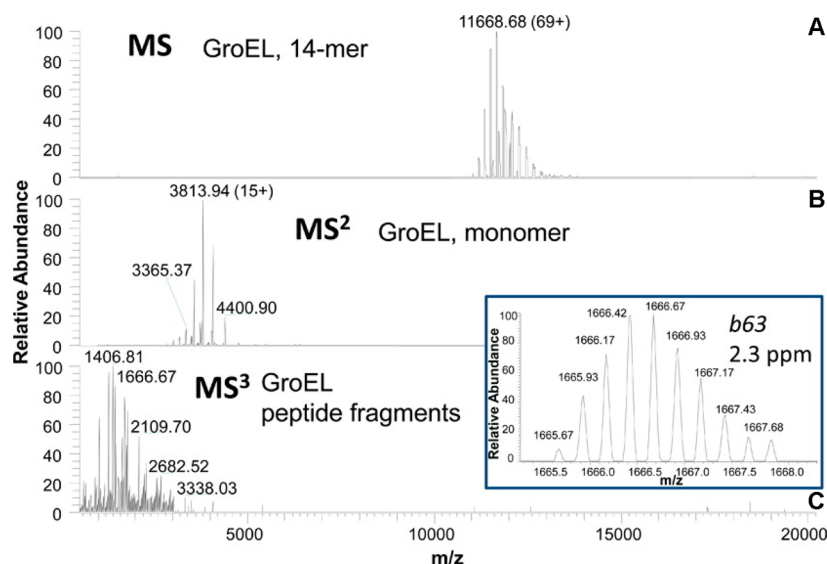


**Figure 9.** GroEL mass spectra acquired under the following conditions: (A) signal obtained by trapping an intact 14-mer GroEL complex in the C-trap; (B) signal of the GroEL monomer subunit obtained upon collisional activation between the funnel exit electrode and inject flatpole. The GroEL monomer ions were accumulated in the C-trap; (C) subunit backbone-level spectrum upon 200 V collisional activation in the HCD cell. The inset shows the signal of one of the GroEL fragment ions (*b*63) identified at a mass measurement accuracy of 2.3 ppm. Reproduced from Belov, M.E., Damoc, E., Denisov, E., Compton, P.D., Horning, S., Makarov, A.A., Kelleher, N.L. *Anal. Chem.* **2013**, *85*, 11163–11173 (ref 246). Copyright 2013 American Chemical Society.

cleavages reflected the interactions of ligands with the protein, either via suppressing fragmentation from the formation of stabilizing interactions between the ligand and protein or by enhancing fragmentation owing to disruption of stabilizing noncovalent interactions. Using this UVPD strategy, complexes of myoglobin/heme,<sup>261,262</sup> eIF4E/m<sup>7</sup>GTP,<sup>261</sup> and peptidyl-prolyl *cis*–*trans* isomerase 1/C-terminal domain of RNA polymerase II (CTD) peptide<sup>261</sup> were examined. The UVPD method was also extended to examine several simple protein complexes, including beta-lactoglobulin dimers and insulin hexamers.<sup>261</sup> The UVPD fragmentation trends appear to reflect less dependence on side-chain interactions and more dependence on the engagement of secondary and tertiary interactions with amide hydrogens (i.e., distinction between loop and helical regions).<sup>261</sup> With respect to the UVPD patterns, backbone cleavages were enhanced at those positions for which the amides were not involved in hydrogen bonding interactions as shown for myoglobin.<sup>261,262</sup> More recently UVPD was used to characterize binary and ternary protein–ligand complexes comprised of dihydrofolate reductase (DHFR) and cofactor NADPH and inhibitor methotrexate (MTX).<sup>263</sup> The resulting UVPD mass spectra of the native complexes gave numerous diagnostic product ions that provided 80% sequence coverage of DHFR, in addition to many fragment ions that retained the NADPH or MTX ligands.<sup>263</sup> The collection of holo (ligand-containing) and apo (ligand-free) product ions offered a means to determine the binding site of each ligand. Comparisons of the fragmentation maps for the various complexes (DHFR alone versus DHFR/NADPH complex versus DHFR/methotrexate complex versus ternary DHFR/NADPH/methotrexate complex) showed significant variations in fragmentation efficiency that were attributed to structural changes.<sup>263</sup> Figure 8 shows cleavage maps across the entire backbone of DHFR (starting with the N-terminus on the left and extending to the C-terminus on the right), with the fragmentation yield measured as a function of the protein sequence. In essence, backbone cleavages were enhanced in the more flexible regions

of the protein, and backbone cleavages were reduced in regions that were “shielded” by the ligand in a way suggestive of formation of new stabilizing intramolecular interactions.<sup>263</sup>

In a look to the future of tandem mass spectrometry in structural biology, a Q-Exactive mass spectrometer was modified to afford high efficiency transfer of large macromolecules into the gas phase. Postsource dissociation was used to disassemble the complexes in a first stage of activation, followed by HCD to sequence the constituent proteins in a second energization step to produce *b*/*y* sequence ions from the proteins.<sup>246</sup> This innovative two-step interface activation/HCD method was used to analyze complexes up to 800 kDa. Figure 9 shows the successful transfer, trapping, and dissociation of the 14-mer GroEL complex.<sup>246</sup> The 800 kDa complex was initially trapped in the C-trap under gentle activation conditions (Figure 9A), then after gentle activation to cause release of highly charged monomer ions (Figure 9B). Figure 9C shows the fragmentation pattern of GroEL, with the inset revealing one of the fully resolved multiply charged fragment ions. As typical for top-down analysis of proteins by collisional activation methods, cleavages of the backbone were more prevalent from the terminal ends of each protein, yielding less comprehensive sequence information from the midsection.

## CONCLUSIONS

The breadth and depth of applications of tandem mass spectrometry for analysis of peptides and proteins underscores the enormous impact of ion activation methods. The ability to sequence peptides and proteins, map their post-translational modifications, identify thousands of peptides in incredibly complex mixtures (and use them to identify proteins), and to dissect intact proteins and even protein complexes is derived from production of meaningful fragmentation patterns. Collisional activation methods have the longest and richest track record, but the entire field has been revitalized and experienced unprecedented growth into new areas since the development of alternative activation techniques, including ones using

electrons, photons, and surfaces, to add more energy to ions or access different activation pathways. Looking ahead, there remain numerous hurdles to overcome as even more complicated biological problems are addressed. Some of these challenges are related to the activation methods themselves, and others arise from affiliated mass spectrometry techniques. Activation methods that can transfer high energy to increasingly large ions and result in high conversion efficiencies of precursors to products is one obvious area for development. As this goal is attained, even greater improvements in the accuracy and resolution of mass analyzers, in addition to more sensitive ion detectors with larger dynamic range, will be essential to increase confidence in assignment of fragment ions. Improvement of the already sophisticated algorithms for facilitating interpretation of spectra is a key goal moving forward, including ones that enhance the ability to exploit de novo methods. Incredible high-throughput data collection and processing methods are already widely implemented, but innovative advances in sample processing, separation methods, and computational power will be needed as interest in cataloging peptides and proteins shifts to protein complexes, macromolecular assemblies, and interactomics.

## AUTHOR INFORMATION

### Corresponding Author

\*Phone: 512-471-9928. E-mail: [jbrodbelt@cm.utexas.edu](mailto:jbrodbelt@cm.utexas.edu).

### Notes

The authors declare no competing financial interest.

### Biography

Jennifer S. Brodbelt earned her B.S in chemistry from the University of Virginia and her Ph.D. in 1988 from Purdue University. She pursued postdoctoral research at the University of California at Santa Barbara from 1988 to 1989. In 1989, she joined the faculty at the University of Texas at Austin where she is currently a professor and the Norman Hackerman Chair in Chemistry. She serves as an associate editor for *Journal of the American Society for Mass Spectrometry* and is currently completing her term as President of the American Society for Mass Spectrometry. Her research focuses on the development of ultraviolet photodissociation mass spectrometry and ion trap mass spectrometry for characterization of peptides, proteins, protein complexes, and lipopolysaccharides.

## ACKNOWLEDGMENTS

Financial support from the National Science Foundation (Grant CHE1402753), the National Institutes of Health (Grants R01-GM103655 and R21 EB018391), and the Welch Foundation (Grant F-1155) are gratefully acknowledged. Julia Aponte is acknowledged for her assistance in creating several figures.

## REFERENCES

- (1) Zhang, Y.; Fonslow, B. R.; Shan, B.; Baek, M.-C.; Yates, J. R. *Chem. Rev.* **2013**, *113*, 2343–2394.
- (2) Angel, T. E.; Aryal, U. K.; Hengel, S. M.; Baker, E. S.; Kelly, R. T.; Robinson, E. W.; Smith, R. D. *Chem. Soc. Rev.* **2012**, *41*, 3912–3923.
- (3) Mayne, J.; Starr, A. E.; Ning, Z.; Chen, R.; Chiang, C. K.; Figeys, D. *Anal. Chem.* **2014**, *86*, 176–195.
- (4) Yates, J. R., III *J. Am. Chem. Soc.* **2013**, *135*, 1629–1640.
- (5) Riley, N. M.; Coon, J. J. *Anal. Chem.* **2015**, DOI: [10.1021/acs.analchem.5b04123](https://doi.org/10.1021/acs.analchem.5b04123).
- (6) Palumbo, A. M.; Smith, S. A.; Kalcic, C. L.; Dantus, M.; Stemmer, P. M.; Reid, G. E. *Mass Spectrom. Rev.* **2011**, *30*, 600–625.
- (7) Jones, A. W.; Cooper, H. J. *Analyst* **2011**, *136*, 3419–3429.
- (8) Cooper, H. J.; Hakansson, K.; Marshall, A. G. *Mass Spectrom. Rev.* **2005**, *24*, 201–222.
- (9) Zhurov, K. O.; Fornelli, L.; Wodrich, M. D.; Laskay, U. A.; Tsybin, Y. O. *Chem. Soc. Rev.* **2013**, *42*, 5014–5023.
- (10) Sarbu, M.; Ghiulai, R. M.; Zamfir, A. D. *Amino Acids* **2014**, *46* (7), 1625–1634.
- (11) Kim, M.-S.; Pandey, A. *Proteomics* **2012**, *12*, 530–542.
- (12) Mikesch, L. M.; Ueberheide, B.; Chi, A.; Coon, J. J.; Syka, J. E. P.; Shabanowitz, J.; Hunt, D. F. *Biochim. Biophys. Acta, Proteins Proteomics* **2006**, *1764*, 1811–1822.
- (13) Wiesner, J.; Premsler, T.; Sickmann, A. *Proteomics* **2008**, *8*, 4466–4483.
- (14) Zhou, Y.; Dong, J.; Vachet, R. W. *Curr. Pharm. Biotechnol.* **2011**, *12*, 1558–1567.
- (15) Coon, J. J. *Anal. Chem.* **2009**, *81*, 3208–3215.
- (16) Brodbelt, J. S. *Chem. Soc. Rev.* **2014**, *43*, 2757–2783.
- (17) Reilly, J. P. *Mass Spectrom. Rev.* **2009**, *28*, 425–447.
- (18) Ly, T.; Julian, R. R. *Angew. Chem., Int. Ed.* **2009**, *48*, 7130–7137.
- (19) Cui, W.; Rohrs, H. W.; Gross, M. L. *Analyst* **2011**, *136*, 3854–3864.
- (20) Catherman, A. D.; Skinner, O. S.; Kelleher, N. L. *Biochem. Biophys. Res. Commun.* **2014**, *445*, 683–693.
- (21) Zhou, H.; Ning, Z.; Starr, A. E.; Abu-Farha, M.; Figeys, D. *Anal. Chem.* **2012**, *84*, 720–734.
- (22) Lanucara, F.; Eyers, C. E. *Mass Spectrom. Rev.* **2013**, *32*, 27–42.
- (23) Cannon, J.; Lohnes, K.; Wynne, C.; Wang, Y. J. *Proteome Res.* **2010**, *9*, 3886–3890.
- (24) Sandra, K.; Moshir, M.; D'hondt, F.; Tuytten, R.; Verleysen, K.; Kas, K.; Francois, I.; Sandra, P. J. *Chromatogr. B: Anal. Technol. Biomed. Life Sci.* **2009**, *877*, 1019–1039.
- (25) Seidler, J.; Zinn, N.; Boehm, M. E.; Lehmann, W. D. *Proteomics* **2010**, *10*, 634–649.
- (26) Eng, J. K.; McCormack, A. L.; Yates, J. R., III *J. Am. Soc. Mass Spectrom.* **1994**, *5* (11), 976–989.
- (27) Perkins, D. N.; Pappin, D. J. C.; Creasy, D. M.; Cottrell, J. S. *Electrophoresis* **1999**, *20* (18), 3551–3567.
- (28) Xu, H.; Freitas, M. A. *Proteomics* **2009**, *9* (6), 1548–1555.
- (29) Geer, L. Y.; Markey, S. P.; Kowalak, J. A.; Wagner, L.; Xu, M.; Maynard, D. M.; Yang, X.; Shi, W.; Bryant, S. H. J. *Proteome Res.* **2004**, *3* (5), 958–964.
- (30) Craig, R.; Cortens, J. P.; Beavis, R. C. J. *Proteome Res.* **2004**, *3* (6), 1234–1242.
- (31) Bern, M.; Kil, Y. J.; Becker, C. Byonic: Advanced Peptide and Protein Identification Software. In *Current Protocols in Bioinformatics*, John Wiley & Sons Inc.: Somerset, NJ, 2012; Chapter 13:Unit13.20. DOI: [10.1002/0471250953.bi1320s40](https://doi.org/10.1002/0471250953.bi1320s40).
- (32) Cox, J.; Mann, M. *Nat. Biotechnol.* **2008**, *26*, 1367–1372.
- (33) Hughes, C.; Ma, B.; Lajoie, G. A. In *Proteome Bioinformatics*; Hubbard, S. J., Jones, A. R., Eds.; Humana Press: Totowa, NJ, 2010; Vol. 604, pp 105–121.
- (34) Seidler, J.; Zinn, N.; Boehm, M. E.; Lehmann, W. D. *Proteomics* **2010**, *10* (4), 634–649.
- (35) Ma, B.; Zhang, K.; Hendrie, C.; Liang, C.; Li, M.; Doherty-Kirby, A.; Lajoie, G. *Rapid Commun. Mass Spectrom.* **2003**, *17* (20), 2337–2342.
- (36) Frank, A.; Pevzner, P. *Anal. Chem.* **2005**, *77* (4), 964–973.
- (37) Fischer, B.; Roth, V.; Roos, F.; Grossmann, J.; Baginsky, S.; Widmayer, P.; Gruissem, W.; Buhmann, J. M. *Anal. Chem.* **2005**, *77* (22), 7265–7273.
- (38) Mo, L.; Dutta, D.; Wan, Y.; Chen, T. *Anal. Chem.* **2007**, *79* (13), 4870–4878.
- (39) Pan, C.; Park, B. H.; McDonald, W. H.; Carey, P. A.; Banfield, J. F.; VerBerkmoes, N. C.; Hettich, R. L.; Samatova, N. F. A. *BMC Bioinf.* **2010**, *11* (1), 118.
- (40) Vyatkin, K.; Wu, S.; Dekker, L. J. M.; VanDuijn, M. M.; Liu, X.; Tolic, N.; Dvorkin, M.; Alexandrova, S.; Luider, T. M.; Pasa-Tolic, L.; Pevzner, P. A. *J. Proteome Res.* **2015**, *14*, 4450–4462.
- (41) Roepstorff, P.; Fohlman, J. *Biomed. Mass Spectrom.* **1984**, *11*, 601–601.

- (42) McLuckey, S. A. *J. Am. Soc. Mass Spectrom.* **1992**, *3*, 599–614.
- (43) Paizs, B.; Suhai, S. *Mass Spectrom. Rev.* **2005**, *24*, 508–48.
- (44) Mitchell Wells, J.; McLuckey, S. A. In *Methods in Enzymology*; Burlingame, A. L., Ed.; Academic Press: New York, 2005; Vol. 402, pp 148–185.
- (45) Olsen, J. V.; Macek, B.; Lange, O.; Makarov, A.; Horning, S.; Mann, M. *Nat. Methods* **2007**, *4* (9), 709–712.
- (46) Dongre, A. R.; Jones, J. L.; Somogyi, A.; Wysocki, V. H. *J. Am. Chem. Soc.* **1996**, *118*, 8365–8374.
- (47) Wysocki, V. H.; Tsapralis, G.; Smith, L. L.; Breci, L. A. *J. Mass Spectrom.* **2000**, *35*, 1399–1406.
- (48) Zubarev, R. A.; Kelleher, N. L.; McLafferty, J. J. *Am. Chem. Soc.* **1998**, *120*, 3265–3266.
- (49) Zubarev, R. A. *Curr. Opin. Biotechnol.* **2004**, *15*, 12–16.
- (50) Zubarev, R. A. *Mass Spectrom. Rev.* **2003**, *22*, 57–77.
- (51) Syka, J. E. P.; Coon, J. J.; Schroeder, M. J.; Shabanowitz, J.; Hunt, D. F. *Proc. Natl. Acad. Sci. U. S. A.* **2004**, *101*, 9528–9533.
- (52) Coon, J. J.; Shabanowitz, J.; Hunt, D. F.; Syka, J. E. P. *J. Am. Soc. Mass Spectrom.* **2005**, *16*, 880–882.
- (53) Turecek, F. *J. Am. Chem. Soc.* **2003**, *125*, 5954–5963.
- (54) Leymarie, N.; Costello, C. E.; O'Connor, P. B. *J. Am. Chem. Soc.* **2003**, *125*, 8949–8958.
- (55) Simons, J. *Chem. Phys. Lett.* **2010**, *484*, 81–95.
- (56) Lioe, H.; O'Hair, R. A. J. *Anal. Bioanal. Chem.* **2007**, *389*, 1429–1437.
- (57) Ly, T.; Yin, S.; Loo, J. A.; Julian, R. R. *Rapid Commun. Mass Spectrom.* **2009**, *23*, 2099–2101.
- (58) Kalli, A.; Grigorean, G.; Hakansson, K. *J. Am. Soc. Mass Spectrom.* **2011**, *22*, 2209–2221.
- (59) Fung, Y. M. W.; Adams, C. M.; Zubarev, R. A. *J. Am. Chem. Soc.* **2009**, *131*, 9977–9985.
- (60) Horn, D. M.; Ge, Y.; McLafferty, F. W. *Anal. Chem.* **2000**, *72*, 4778–4784.
- (61) Oh, H. B.; McLafferty, F. W. *Bull. Korean Chem. Soc.* **2006**, *27*, 389–394.
- (62) Pitteri, S. J.; Chrisman, P. A.; McLuckey, S. A. *Anal. Chem.* **2005**, *77*, 5662–5669.
- (63) Ledvina, A. R.; McAlister, G. C.; Gardner, M. W.; Smith, S. I.; Madsen, J. A.; Schwartz, J. C.; Stafford, G. C.; Syka, J. E. P.; Brodbelt, J. S.; Coon, J. J. *Angew. Chem., Int. Ed.* **2009**, *48*, 8526–8528.
- (64) Swaney, D. L.; McAlister, G. C.; Wirtala, M.; Schwartz, J. C.; Syka, J. E.; Coon, J. J. *Anal. Chem.* **2007**, *79*, 477–485.
- (65) Mikhailov, V. A.; Cooper, H. J. *J. Am. Soc. Mass Spectrom.* **2009**, *20*, 763–771.
- (66) Mao, Y.; Valeja, S. G.; Rouse, J. C.; Hendrickson, C. L.; Marshall, A. G. *Anal. Chem.* **2013**, *85*, 4239–4246.
- (67) Bourgoin-Voillard, S.; Leymarie, N.; Costello, C. E. *Proteomics* **2014**, *14*, 1174–1184.
- (68) Riley, N. M.; Westphall, M. S.; Coon, J. J. *Anal. Chem.* **2015**, *87*, 7109–7116.
- (69) Budnik, B. A.; Haselmann, K. F.; Zubarev, R. A. *Chem. Phys. Lett.* **2001**, *342*, 299–302.
- (70) Kjeldsen, F.; Silivra, O. A.; Ivonin, I. A.; Haselmann, K. F.; Gorshkov, M.; Zubarev, R. A. *Chem. - Eur. J.* **2005**, *11*, 1803–1812.
- (71) Kjeldsen, F.; Horning, O. B.; Jensen, S. S.; Giessing, A. M. B.; Jensen, O. N. *J. Am. Soc. Mass Spectrom.* **2008**, *19*, 1156–1162.
- (72) Song, H.; Hakansson, K. *Anal. Chem.* **2012**, *84*, 871–876.
- (73) Kalli, A.; Gigorean, G.; Hakansson, K. *J. Am. Soc. Mass Spectrom.* **2011**, *22*, 2209–2221.
- (74) Yoo, H. J.; Wang, N.; Zhuang, S.; Song, H.; Hakansson, K. *J. Am. Chem. Soc.* **2011**, *133*, 16790–16793.
- (75) Hersberger, K. E.; Hakansson, K. *Anal. Chem.* **2012**, *84*, 6370–6377.
- (76) Coon, J. J.; Shabanowitz, J.; Hunt, D. F.; Syka, J. E. P. *J. Am. Soc. Mass Spectrom.* **2005**, *16*, 880–882.
- (77) Huzarska, M.; Ugalde, I.; Kaplan, D. A.; Hartmer, R.; Easterling, M. L.; Polfer, N. C. *Anal. Chem.* **2010**, *82*, 2873–2878.
- (78) Rumachik, N. G.; McAlister, G. C.; Russell, J. D.; Bailey, D. J.; Wenger, C. D.; Coon, J. J. *J. Am. Soc. Mass Spectrom.* **2012**, *23*, 718–727.
- (79) McAlister, G. C.; Russell, J. D.; Rumachik, N. G.; Hebert, A. S.; Syka, J. E. P.; Geer, L. Y.; Westphall, M. S.; Pagliarini, D. J.; Coon, J. J. *Anal. Chem.* **2012**, *84*, 2875–2882.
- (80) Shaw, J. B.; Kaplan, D. A.; Brodbelt, J. S. *Anal. Chem.* **2013**, *85* (9), 4721–4728.
- (81) Riley, N. M.; Rush, M. J. P.; Rose, C. M.; Richards, A. L.; Kwiecien, N. W.; Bailey, D. J.; Hebert, A. S.; Westphall, M. S.; Coon, J. J. *Mol. Cell. Proteomics* **2015**, *14*, 2644–2660.
- (82) Brodbelt, J. S.; Wilson, J. J. *Mass Spectrom. Rev.* **2009**, *28*, 390–424.
- (83) Gardner, M. A.; Ledvina, A. R.; Smith, S.; Madsen, J.; Schwartz, G. C.; Stafford, G. C.; Coon, J. J.; Brodbelt, J. S. *Anal. Chem.* **2009**, *81*, 8109–8118.
- (84) Madsen, J. A.; Gardner, M. W.; Smith, S. I.; Ledvina, A. R.; Coon, J. J.; Schwartz, J. C.; Stafford, G. C.; Brodbelt, J. S. *Anal. Chem.* **2009**, *81*, 8677–8686.
- (85) Ledvina, A. R.; Lee, M. V.; McAlister, G. C.; Westphall, M. S.; Coon, J. J. *Anal. Chem.* **2012**, *84*, 4513–4519.
- (86) Thompson, M. S.; Cui, W. D.; Reilly, J. P. *Angew. Chem., Int. Ed.* **2004**, *43*, 4791–4794.
- (87) Madsen, J. A.; Boutz, D. R.; Brodbelt, J. S. *J. Proteome Res.* **2010**, *9*, 4205–4214.
- (88) Kalcic, C. L.; Gunaratne, T. C.; Jones, A. D.; Dantus, M.; Reid, G. E. *J. Am. Chem. Soc.* **2009**, *131*, 940–942.
- (89) Yeh, G. K.; Sun, Q. Y.; Meneses, C.; Julian, R. R. *J. Am. Soc. Mass Spectrom.* **2009**, *20*, 385–393.
- (90) Park, S.; Ahn, W. K.; Lee, S.; Han, S. Y.; Rhee, B. K.; Oh, H. B. *Rapid Commun. Mass Spectrom.* **2009**, *23*, 3609–3620.
- (91) Lai, C. K.; Ng, D. C. M.; Pang, H. F.; Le Blanc, J. C. Y.; Hager, J. W.; Fang, D.-C.; Cheung, A. S. C.; Chu, I. K. *Rapid Commun. Mass Spectrom.* **2013**, *27*, 1119–1127.
- (92) Wilson, J. J.; Brodbelt, J. S. *Anal. Chem.* **2007**, *79*, 7883–7892.
- (93) O'Brien, J. O.; Pruet, J.; Brodbelt, J. S. *Anal. Chem.* **2013**, *85*, 7391–7397.
- (94) Enjalbert, Q.; Girod, M.; Simon, R.; Jeudy, J.; Chirot, F.; Salvador, A.; Antoine, R.; Dugourd, P.; Lemoine, J. *Anal. Bioanal. Chem.* **2013**, *405*, 2321–2331.
- (95) Girod, M.; Biarc, J.; Enjalbert, Q.; Salvador, A.; Antoine, R.; Dugourd, P.; Lemoine, J. *Analyst* **2014**, *139*, 5523–5530.
- (96) Cui, W.; Thompson, M. S.; Reilly, J. P. *J. Am. Soc. Mass Spectrom.* **2005**, *16*, 1384–1398.
- (97) Thompson, M. S.; Cui, W.; Reilly, J. P. *J. Am. Soc. Mass Spectrom.* **2007**, *18*, 1439–1452.
- (98) Parthasarathi, R.; He, Y.; Reilly, J. P.; Raghavachari, K. *J. Am. Chem. Soc.* **2010**, *132*, 1606–1610.
- (99) He, Y.; Webber, N.; Reilly, J. P. *J. Am. Soc. Mass Spectrom.* **2013**, *24*, 675–683.
- (100) Webber, N.; He, Y.; Reilly, J. P. *J. Am. Soc. Mass Spectrom.* **2014**, *25*, 196–203.
- (101) Madsen, J. A.; Cheng, R. R.; Kaoud, T. S.; Dalby, K. N.; Makarov, D. E.; Brodbelt, J. S. *Chem. - Eur. J.* **2012**, *18*, 5374–5383.
- (102) Woody, R. W.; Koslowski, A. *Biophys. Chem.* **2002**, *101*–102, 535–551.
- (103) Madsen, J.; Boutz, D.; Brodbelt, J. S. *J. Proteome Res.* **2010**, *9*, 4205–4214.
- (104) Luo, Y.; Yogesha, S. D.; Cannon, J. R.; Yan, W.; Ellington, A. D.; Brodbelt, J. S.; Zhang, Y. *ACS Chem. Biol.* **2013**, *8*, 2042–2052.
- (105) Madsen, J.; Kaoud, T.; Dalby, K.; Brodbelt, J. S. *Proteomics* **2011**, *11*, 1329–1334.
- (106) Han, S.-W.; Lee, S.-W.; Bahar, O.; Schwessinger, B.; Robinson, M. R.; Shaw, J. B.; Madsen, J. A.; Brodbelt, J. S.; Ronald, P. A. *Nat. Commun.* **2012**, *3*, 1153.
- (107) Robinson, M.; Moore, K.; Brodbelt, J. S. *J. Am. Soc. Mass Spectrom.* **2014**, *25* (8), 1461–1471.
- (108) Pruitt, R. N.; Schwessinger, B.; Joe, A.; Thomas, N.; Liu, F.; Albert, M.; Robinson, M. R.; Chan, L. J. G.; Luu, D. D.; Chen, H.;

- Bahar, O.; Daudi, A.; Veleeschauwer, D.; Caddell, D.; Xhang, W.; Zhao, X.; Li, X.; Heaslewood, J. L.; Ruan, D.; Majumder, D.; Chern, M.; Kalbacher, H.; Midha, S.; Patil, P. B.; Sonti, R. V.; Petzold, C. J.; Liu, C.; Brodbelt, J. S.; Felix, G.; Ronald, P. C. *ScienceAdvances* **2015**, *1*, e1500245.
- (109) Madsen, J. A.; Ko, B. Y.; Robotham, S. S.; Xu, H.; Horton, A. P.; Iwashkiw, J. A.; Shaw, J. B.; Feldman, M. F.; Brodbelt, J. S. *Anal. Chem.* **2013**, *85*, 9253–9261.
- (110) Ko, B. J.; Brodbelt, J. S. *Int. J. Mass Spectrom.* **2015**, *377*, 385–392.
- (111) Robinson, M. R.; Madsen, J. A.; Brodbelt, J. S. *Anal. Chem.* **2012**, *84*, 2433–2439.
- (112) Madsen, J. A.; Xu, H.; Robinson, M. R.; Horton, A. P.; Shaw, J. B.; Giles, D. K.; Kaoud, T. S.; Dalby, K. N.; Trent, M. S.; Brodbelt, J. S. *Mol. Cell. Proteomics* **2013**, *12* (9), 2604–2614.
- (113) Greer, S. M.; Cannon, J. R.; Brodbelt, J. S. *Anal. Chem.* **2014**, *86*, 12285–12290.
- (114) Vasicek, L.; Brodbelt, J. S. *Anal. Chem.* **2010**, *82* (22), 9441–9446.
- (115) Greer, S. M.; Parker, W. R.; Brodbelt, J. S. *J. Proteome Research* **2015**, *14*, 2626–2632.
- (116) Shaw, J. B.; Li, W.; Holden, D. D.; Zhang, Y.; Griep-Raming, J.; Fellers, R. T.; Early, B. P.; Thomas, P. M.; Kelleher, N. L.; Brodbelt, J. S. *J. Am. Chem. Soc.* **2013**, *135*, 12646–12651.
- (117) Ellefson, J. W.; Meyer, A. J.; Hughes, R. A.; Cannon, J.; Brodbelt, J. S.; Ellington, A. D. *Nat. Biotechnol.* **2014**, *32*, 97–101.
- (118) Cannon, J. R.; Cammarata, M. B.; Robotham, S. A.; Cotham, V. C.; Shaw, J. B.; Fellers, R. T.; Early, B. P.; Thomas, P. M.; Kelleher, N. L.; Brodbelt, J. S. *Anal. Chem.* **2014**, *86*, 2185–2192.
- (119) Cannon, J.; Kluwe, C.; Ellington, A.; Brodbelt, J. S. *Proteomics* **2014**, *14*, 1165–1173.
- (120) Thyer, R.; Robotham, S. A.; Brodbelt, J. S.; Ellington, A. *J. Am. Chem. Soc.* **2015**, *137*, 46–49.
- (121) Cannon, J. S.; Martinez Fonts, K.; Robotham, S. A.; Matouschek, A.; Brodbelt, J. S. *Anal. Chem.* **2015**, *87*, 1812–1820.
- (122) Cannon, J. R.; Holden, D. D.; Brodbelt, J. S. *Anal. Chem.* **2014**, *86*, 10970–10977.
- (123) Oh, J. Y.; Moon, J. H.; Kim, M. S. *Rapid Commun. Mass Spectrom.* **2004**, *18*, 2706–2712.
- (124) Oh, J. Y.; Moon, J. H.; Kim, M. S. *J. Mass Spectrom.* **2005**, *40*, 899–907.
- (125) Diedrich, J. K.; Julian, R. R. *Anal. Chem.* **2011**, *83*, 6818–6826.
- (126) Agarwal, A.; Diedrich, J. K.; Julian, R. R. *Anal. Chem.* **2011**, *83*, 6455–6458.
- (127) Tao, Y.; Quebbermann, N. R.; Julian, R. R. *Anal. Chem.* **2012**, *84*, 6814–6820.
- (128) Zhang, X.; Li, H.; Moore, B.; Wongkongkathep, P.; Ogorzalek Loo, R. R.; Loo, J. A.; Julian, R. R. *Rapid Commun. Mass Spectrom.* **2014**, *28*, 2729–2734.
- (129) Tao, Y.; Julian, R. R. *Anal. Chem.* **2014**, *86*, 9733–9741.
- (130) Hamdy, O. M.; Lam, S.; Julian, R. R. *Anal. Chem.* **2014**, *86*, 3653–3658.
- (131) Bellina, B.; Brown, J. M.; Ujma, J.; Murray, P.; Giles, K.; Morris, M.; Compagnon, I.; Barran, P. E. *Analyst* **2014**, *139*, 6348–6351.
- (132) Cotham, V. C.; Wine, Y.; Brodbelt, J. S. *Anal. Chem.* **2013**, *85*, 5577–5585.
- (133) O'Brien, J. P.; Mayberry, L. K.; Murphy, P. A.; Browning, K. S.; Brodbelt, J. S. *J. Proteome Research* **2013**, *12*, 5867–5877.
- (134) Robotham, S. A.; Kluwe, C.; Cannon, J. R.; Ellington, A.; Brodbelt, J. S. *Anal. Chem.* **2013**, *85*, 9832–9838.
- (135) Aponte, J.; Vasicek, L.; Swaminathan, J.; Xu, H.; Koag, M. C.; Lee, S.; Brodbelt, J. S. *Anal. Chem.* **2014**, *86*, 6237–6244.
- (136) McCormack, A. L.; Jones, J. L.; Wysocki, V. H. *J. Am. Soc. Mass Spectrom.* **1992**, *3*, 859–862.
- (137) Wysocki, V. H.; Joyce, K. E.; Jones, C. M.; Beardsley, R. L. *J. Am. Soc. Mass Spectrom.* **2008**, *19*, 190–208.
- (138) Zhou, M.; Jones, C. M.; Wysocki, V. H. *Anal. Chem.* **2013**, *85*, 8262–8267.
- (139) Zhou, M.; Wysocki, V. H. *Acc. Chem. Res.* **2014**, *47*, 1010–1018.
- (140) Ma, X.; Zhou, M.; Wysocki, V. H. *J. Am. Soc. Mass Spectrom.* **2014**, *25*, 368–379.
- (141) Ma, X.; Lai, L. B.; Lai, S. M.; Tanimoto, A.; Foster, M. P.; Wysocki, V. H.; Gopalan, V. *Angew. Chem., Int. Ed.* **2014**, *53*, 11483–11487.
- (142) Quintyn, Q.; Yan, J.; Wysocki, V. H. *Chem. Biol.* **2015**, *22*, 583–592.
- (143) Quintyn, R. S.; Harvey, S. R.; Wysocki, V. H. *Analyst* **2015**, *140*, 7012–7019.
- (144) Quintyn, R. S.; Zhou, M.; Yan, J.; Wysocki, V. H. *Anal. Chem.* **2015**, *87*, 11879–11886.
- (145) Misharin, A. S.; Silivra, O. A.; Kjeldsen, F.; Zubarev, R. A. *Rapid Commun. Mass Spectrom.* **2005**, *19*, 2163–2171.
- (146) Berkout, V. D. *Anal. Chem.* **2009**, *81*, 725–731.
- (147) Cook, S. L.; Collin, O. L.; Jackson, G. P. *J. Mass Spectrom.* **2009**, *44*, 1211–1223.
- (148) Cook, S. L.; Jackson, G. P. *J. Am. Soc. Mass Spectrom.* **2011**, *22*, 1088–1099.
- (149) Cook, S. L.; Zimmermann, C. M.; Singer, D.; Fedorova, M.; Hoffmann, R.; Jackson, G. P. *J. Mass Spectrom.* **2012**, *47*, 786–794.
- (150) Hoffmann, W. D.; Jackson, G. P. *J. Am. Soc. Mass Spectrom.* **2014**, *25*, 1939–1943.
- (151) Chingin, K.; Makarov, A.; Denisov, E.; Rebrov, O.; Zubarev, R. A. *Anal. Chem.* **2014**, *86*, 372–379.
- (152) Antoine, A.; Joly, L.; Tabarin, T.; Broyer, M.; Dugourd, J.; Lemoine, J. *Rapid Commun. Mass Spectrom.* **2007**, *21*, 265–268.
- (153) Larraillet, V.; Antoine, R.; Dugourd, P.; Lemoine, J. *Anal. Chem.* **2009**, *81*, 8410–8416.
- (154) Larraillet, V.; Vorobyev, A.; Brunet, C.; Lemoine, J.; Tsybin, Y. O.; Antoine, R.; Dugourd, P. *J. Am. Soc. Mass Spectrom.* **2010**, *21*, 670–680.
- (155) Shaw, J.; Madsen, J.; Xu, H.; Brodbelt, J. S. *J. Am. Soc. Mass Spectrom.* **2012**, *23*, 1707–1715.
- (156) Shao, C.; Zhang, Y.; Sun, W. *J. Proteomics* **2014**, *109*, 26–37.
- (157) Michalski, A.; Neuhauser, N.; Cox, J.; Mann, M. *J. Proteome Res.* **2012**, *11*, 5479–5491.
- (158) Tabb, D. L.; Smith, L. L.; Breci, L. A.; Wysocki, V. H.; Lin, D.; Yates, J. R., 3rd. *Anal. Chem.* **2003**, *75*, 1155–1163.
- (159) Huang, Y.; Triscari, J. M.; Tseng, G. C.; Pasa-Tolic, L.; Lipton, M. S.; Smith, R. D.; Wysocki, V. H. *Anal. Chem.* **2005**, *77*, 5800–5803.
- (160) Mous, L.; Aubagnac, J. L.; Martinez, J.; Enjalbal, C. *J. Proteome Research* **2007**, *6*, 1378–1391.
- (161) Good, D. M.; Wirtala, M.; McAlister, G. C.; Coon, J. J. *Mol. Cell. Proteomics* **2007**, *6*, 1942–1951.
- (162) Chalkley, R. J.; Medzihradsky, K. F.; Lynn, A. J.; Baker, P. R.; Burlingame, A. L. *Anal. Chem.* **2010**, *82*, 579–84.
- (163) Li, W.; Song, C.; Bailey, D. J.; Tseng, G. C.; Coon, J. J.; Wysocki, V. H. *Anal. Chem.* **2011**, *83*, 9540–9545.
- (164) Chalkley, R. J. *Methods Mol. Biol.* **2013**, *1007*, 173–182.
- (165) Savitski, M. M.; Kjeldsen, F.; Nielsen, M. L.; Zubarev, R. A. *Angew. Chem., Int. Ed.* **2006**, *45*, 5301–5303.
- (166) Liu, X.; Li, Y. F.; Bohrer, B. C.; Arnold, R. J.; Radivojac, P.; Tang, H.; Reilly, J. P. *Int. J. Mass Spectrom.* **2011**, *308*, 142–154.
- (167) Michalski, A.; Cox, J.; Mann, M. *J. Proteome Res.* **2011**, *10*, 1785–1793.
- (168) Chapman, J. D.; Goodlett, D. R.; Masselon, C. D. *Mass Spectrom. Rev.* **2014**, *33*, 452–470.
- (169) Stahl, D. C.; Swiderek, K. M.; Davis, M. T.; Lee, T. D. *J. Am. Soc. Mass Spectrom.* **1996**, *7*, 532–540.
- (170) Wang, N.; Li, L. *Anal. Chem.* **2008**, *80*, 4696–4710.
- (171) Lange, V.; Picotti, P.; Domon, B.; Aebersold, R. *Mol. Syst. Biol.* **2008**, *4*, 222.
- (172) Peterson, A. C.; Russell, J. D.; Bailey, D. J.; Westphall, M. S.; Coon, J. J. *Mol. Cell. Proteomics* **2012**, *11*, 1475–1488.
- (173) Gallien, S.; Bourmaud, A.; Kim, S. Y.; Domon, B. *J. Proteomics* **2014**, *100*, 147–159.

- (174) Masselon, C.; Anderson, G. A.; Harkewicz, R.; Bruce, J. E.; Pasa-Tolic, L.; Smith, R. D. *Anal. Chem.* **2000**, *72*, 1918–1924.
- (175) Venable, J. D.; Dong, M. Q.; Wohlschlegel, J.; Dillin, A.; Yates, J. R., III *Nat. Methods* **2004**, *1* (1), 39–45.
- (176) Kiyonami, R.; Schoen, A.; Prakash, A.; Peterman, S.; Zabrouskov, V.; Picotti, P.; Aebersold, R.; Huhmer, A.; Domon, B. *Mol. Cell. Proteomics* **2011**, *10*, M110.002931.
- (177) Bateman, N. W.; Goulding, S. P.; Shulman, N. J.; Gadok, A. K.; Szumlanski, K. K.; MacCoss, M. J.; Wu, C. C. *Mol. Cell. Proteomics* **2014**, *13*, 329–338.
- (178) Bauer, M.; Ahrne, E.; Baron, A. P.; Glatter, T.; Fava, L. L.; Santamaria, A.; Nigg, E. A.; Schmidt, A. *J. Proteome Res.* **2014**, *13*, 5973–5988.
- (179) Canterbury, J. D.; Merrihew, G. E.; MacCoss, M. J.; Goodlett, D. R.; Shaffer, S. A. *J. Am. Soc. Mass Spectrom.* **2014**, *25*, 2048–2059.
- (180) Savitski, M. M.; Nielsen, M. L.; Zubarev, R. A. *Mol. Cell. Proteomics* **2005**, *4*, 1180–1188.
- (181) Molina, H.; Matthiesen, R.; Kandasamy, K.; Pandey, A. *Anal. Chem.* **2008**, *80*, 4825–4835.
- (182) Swaney, D. L.; McAlister, G. C.; Coon, J. J. *Nat. Methods* **2008**, *5*, 959–964.
- (183) Kim, S.; Mischerikow, N.; Bandeira, N.; Navarro, J. D.; Wich, L.; Mohammed, S.; Heck, A. J.; Pevzner, P. A. *Mol. Cell. Proteomics* **2010**, *9*, 2840–2852.
- (184) Shen, Y.; Tolic, N.; Xie, F.; Zhao, R.; Purvine, S. O.; Schepmoes, A. A.; Moore, R. J.; Anderson, G. A.; Smith, R. D. *J. Proteome Res.* **2011**, *10*, 3929–3943.
- (185) Zhao, P.; Viner, R.; Teo, C. F.; Boons, G.-J.; Horn, D. M.; Wells, L. *J. Proteome Res.* **2011**, *10*, 4088–4104.
- (186) Frese, C. K.; Altelaar, A. F. M.; Hennrich, M. L.; Nolting, D.; Zeller, M.; Griep-Raming, J.; Heck, A. J. R.; Mohammed, S. *J. Proteome Res.* **2011**, *10*, 2377–2388.
- (187) Frese, C. K.; Altelaar, A. F. M.; van den Toorn, H.; Nolting, D.; Griep-Raming, J.; Heck, A. J. R.; Mohammed, S. *Anal. Chem.* **2012**, *84*, 9668–9673.
- (188) Vandenbogaert, M.; Hourdel, V.; Jardin-Mathe, O.; Bigeard, J.; Bonhomme, L.; Legros, V.; Hirt, H.; Schwikowski, B.; Pflieger, D. *J. Proteome Res.* **2012**, *11*, 5695–5703.
- (189) Hansen, T. A.; Sylvestre, M.; Jensen, O. N.; Kjeldsen, F. *Anal. Chem.* **2012**, *84*, 9694–9.
- (190) Sweet, S. M. M.; Creese, A. J.; Cooper, H. J. *Anal. Chem.* **2006**, *78*, 7563–7569.
- (191) Singh, C.; Zampronio, C. G.; Creese, A. J.; Cooper, H. J. *J. Proteome Res.* **2012**, *11*, 4517–4525.
- (192) Sweet, S. M. M.; Bailey, C. M.; Cunningham, D. L.; Heath, J. K.; Cooper, H. J. *Mol. Cell. Proteomics* **2009**, *8*, 904–912.
- (193) Steentoft, C.; Vakhrushev, S. Y.; Vester-Christensen, M. B.; Schjoldager, K. T.-B. G.; Kong, Y.; Bennett, E. P.; Mandel, U.; Wandall, H.; Lavery, S. B.; Clausen, H. *Nat. Methods* **2011**, *8*, 977–982.
- (194) Bourgoin-Voillard, S.; Leymarie, N.; Costello, C. E. *Proteomics* **2014**, *14*, 1174–1184.
- (195) Frese, C. K.; Altelaar, A. F.; van den Toorn, H.; Nolting, D.; Griep-Raming, J.; Heck, A. J.; Mohammed, S. *Anal. Chem.* **2012**, *84*, 9668–9673.
- (196) Frese, C. K.; Zhou, H.; Taus, T.; Altelaar, A. F.; Mechtler, K.; Heck, A. J.; Mohammed, S. *J. Proteome Res.* **2013**, *12*, 1520–1525.
- (197) Liu, F.; van Breukelen, B.; Heck, A. J. *Mol. Cell. Proteomics* **2014**, *13*, 2776–2786.
- (198) Mommen, G. P.; Frese, C. K.; Meiring, H. D.; van Gaans-van den Brink, J.; de Jong, A. P.; van Els, C. A.; Heck, A. J. *Proc. Natl. Acad. Sci. U. S. A.* **2014**, *111*, 4507–4512.
- (199) Kocher, T.; Pichler, P.; Swart, R.; Mechtler, K. *Nat. Protoc.* **2012**, *7*, 882–890.
- (200) Yamana, R.; Iwasaki, M.; Wakabayashi, M.; Nakagawa, M.; Yamanka, S.; Ishihama, Y. *J. Proteome Res.* **2013**, *12*, 214–221.
- (201) Pirmoradian, M.; Budamgunta, H.; Chinglin, K.; Zhang, B.; Astorga-Wells, J.; Zubarev, R. *Mol. Cell. Proteomics* **2013**, *12*, 3330–3338.
- (202) Sharma, K.; D'Souza, R. C. J.; Tyanova, S.; Schaab, C.; Wisniewski, J. R.; Cox, J.; Mann, M. *Cell Rep.* **2014**, *8*, 1583–1594.
- (203) Hebert, A. S.; Richards, A. L.; Bailey, D. J.; Ulbrich, A.; Coughlin, E. E.; Westphall, M. S.; Coon, J. J. *Mol. Cell. Proteomics* **2014**, *13*, 339–347.
- (204) Sun, L.; Zhu, G.; Mou, S.; Zhao, Y.; Champion, M. M.; Dovichi, N. J. *J. Chrom. A* **2014**, *1359*, 303–308.
- (205) Ludwig, K. R.; Sun, L.; Zhu, G.; Dovichi, N. J.; Hummon, A. B. *Anal. Chem.* **2015**, *87*, 9532–9537.
- (206) Phanstiel, D. H.; Brumbaugh, J.; Wenger, C. D.; Tian, S.; Probasco, M. D.; Bailey, D. J.; Swaney, D. L.; Tervo, M. A.; Bolin, J. M.; Ruotti, V.; Stewart, R.; Thomson, J. A.; Coon, J. J. *Nat. Methods* **2011**, *8*, 821–827.
- (207) Sasaki, K.; Osaki, T.; Minamino, N. *Mol. Cell. Proteomics* **2013**, *12*, 700–709.
- (208) Kelleher, N. L.; Thomas, P. M.; Ntai, I.; Compton, P. D.; LeDuc, R. D. *Expert Rev. Proteomics* **2014**, *11*, 649–651.
- (209) Peng, Y.; Ayaz-Guner, S.; Yu, D.; Ge, Y. *Proteomics: Clin. Appl.* **2014**, *8*, 554–568.
- (210) Reid, G. E.; Wu, J.; Chrisman, P. A.; Wells, J. M.; McLuckey, S. A. *Anal. Chem.* **2001**, *73*, 3274–3281.
- (211) Cobb, J. S.; Easterling, M. L.; Agar, J. N. *J. Am. Soc. Mass Spectrom.* **2010**, *21*, 949–959.
- (212) Fornelli, L.; Parra, J.; Hartmer, R.; Stoermer, C.; Lubeck, M.; Tsybin, Y. O. *Anal. Bioanal. Chem.* **2013**, *405*, 8505–8514.
- (213) Peng, Y.; Chen, X.; Sato, T.; Rankin, S. A.; Tsuji, R. F.; Ge, Y. *Anal. Chem.* **2012**, *84*, 3339–3346.
- (214) Brunner, A. M.; Lossi, P.; Liu, F.; Huguet, R.; Mullen, C.; Yamashita, M.; Zabrouskov, V.; Makarov, A.; Altelaar, A. F. M.; Heck, A. J. R. *Anal. Chem.* **2015**, *87*, 4152–4158.
- (215) Skinner, O. S.; Catherman, A. D.; Early, B. P.; Thomas, P. M.; Compton, P. D.; Kelleher, N. L. *Anal. Chem.* **2014**, *86*, 4627–4634.
- (216) Fornelli, L.; Damoc, E.; Thomas, P. M.; Kelleher, N. L.; Aizikov, K.; Denisov, E.; Makarov, A.; Tsybin, Y. O. *Mol. Cell. Proteomics* **2012**, *11*, 1758–1767.
- (217) Wu, C.; Tran, J. C.; Zamdborg, L.; Durbin, K.; Li, M.; Ahlf, D. R.; Early, B. P.; Thomas, P. M.; Sweedler, J. V.; Kelleher, N. L. *Nat. Methods* **2012**, *9*, 822–824.
- (218) Fornelli, L.; Ayoub, D.; Aizikov, K.; Beck, A.; Tsybin, Y. O. *Anal. Chem.* **2014**, *86*, 3005–3012.
- (219) Wang, D.; Wynne, C.; Gu, F.; Becker, C.; Zhao, J.; Mueller, H.-M.; Li, H.; Shameem, M.; Liu, Y.-H. *Anal. Chem.* **2015**, *87*, 914–921.
- (220) Tran, B. Q.; Barton, C.; Feng, J.; Sandjong, A.; Yoon, S. H.; Awasthi, S.; Liang, D.; Khan, M. M.; Kilgour, D. P.; Goo, Y. A. *J. Proteomics* **2015**, DOI: 10.1016/j.jprot.2015.10.021.
- (221) Ansong, C.; Wu, S.; Meng, D.; Liu, X.; Brewer, H. M.; Deatherage Kaiser, B. L.; Nakayasu, E. S.; Cort, J. R.; Pevzner, P.; Smith, R. D.; Heffron, F.; Adkins, J. N.; Pasa-Tolic, L. *Proc. Natl. Acad. Sci. U. S. A.* **2013**, *110*, 10153–10158.
- (222) Tran, J. C.; Zamdborg, L.; Ahlf, D. R.; Lee, J. E.; Catherman, A. D.; Durbin, K. R.; Tipton, J. D.; Vellaichamy, A.; Kellie, J. F.; Li, M.; Wu, C.; Sweet, S. M. M.; Early, B. P.; Siuti, N.; LeDuc, R. D.; Compton, P. D.; Thomas, P. M.; Kelleher, N. L. *Nature* **2011**, *480*, 254–258.
- (223) Catherman, A. D.; Durbin, K. R.; Ahlf, D. R.; Early, B. P.; Fellers, R. T.; Tran, J. C.; Thomas, P. M.; Kelleher, N. L. *Mol. Cell. Proteomics* **2013**, *12*, 3465–3473.
- (224) Sun, L.; Knierman, M. D.; Zhu, G.; Dovichi, N. J. *Anal. Chem.* **2013**, *85*, 5989–5995.
- (225) Zhao, Y.; Riley, N. M.; Sun, L.; Hebert, A.; Yan, X.; Westphall, M. S.; Rush, M. J. P.; Zhu, G.; Champion, M. M.; Medi, F. M.; DiGiuseppe, P. A.; Coon, J. J.; Dovichi, N. J. *Anal. Chem.* **2015**, *87*, 5422–5429.
- (226) Li, Y.; Compton, P. D.; Tran, J. C.; Ntai, I.; Kelleher, N. L. *Proteomics* **2014**, *14*, 1158–1164.
- (227) Han, X.; Wang, Y.; Aslanian, A.; Bern, M.; Lavalley-Adam, M.; Yates, J. R., 3rd *Anal. Chem.* **2014**, *86*, 11006–12.
- (228) Zinnel, N. F.; Pai, P.-J.; Russell, D. H. *Anal. Chem.* **2012**, *84*, 3390–3397.

- (229) Durbin, K. R.; Skinner, O. S.; Fellers, R. T.; Kelleher, N. L. *J. Am. Soc. Mass Spectrom.* **2015**, *26*, 782–787.
- (230) Molden, R. C.; Garcia, B. A. *Curr. Protoc. Protein Sci.* **2014**, *77*, 23.7.1–23.7.28.
- (231) Kalli, A.; Sweredoski, M. J.; Hess, S. *Anal. Chem.* **2013**, *85*, 3501–3507.
- (232) Moradian, A.; Kalli, A.; Sweredoski, M. J.; Hess, S. *Proteomics* **2014**, *14*, 489–497.
- (233) Sidoli, S.; Schwammle, V.; Ruminowicz, C.; Hansen, T. A.; Wu, X.; Helin, K.; Jensen, O. N. *Proteomics* **2014**, *14*, 2200–2211.
- (234) Tvardovskiy, A.; Wrzesinski, K.; Sidoli, S.; Fey, S. J.; Rogowska-Wrzesinska, A.; Jensen, O. N. *Mol. Cell. Proteomics* **2015**, *14*, 3142–3153, DOI: 10.1074/mcp.M115.048975.
- (235) Sidoli, S.; Lin, S.; Karch, K. R.; Garcia, B. A. *Anal. Chem.* **2015**, *87*, 3129–3133.
- (236) Sweredoski, M. J.; Moradian, A.; Raedle, M.; Franco, C.; Hess, S. *Anal. Chem.* **2015**, *87*, 8360–8366.
- (237) Valkevich, E. M.; Sanchez, N. A.; Ge, Y.; Strieter, E. R. *Biochemistry* **2014**, *53*, 4979–4989.
- (238) Lee, A. E.; Castaneda, C.; Wang, Y.; Fushman, D.; Fenselau, C. *J. Mass Spectrom.* **2014**, *49*, 1272.
- (239) Konermann, L.; Vahidi, S.; Sowole, M. A. *Anal. Chem.* **2014**, *86*, 213–232.
- (240) Benesch, J. L.; Ruotolo, B. T. *Curr. Opin. Struct. Biol.* **2011**, *21*, 641–649.
- (241) Marcoux, J.; Robinson, C. V. *Structure* **2013**, *21*, 1541–1550.
- (242) Heck, A. J. R. *Nat. Methods* **2008**, *5*, 927–933.
- (243) Snijder, J.; Rose, R. J.; Veessler, D.; Johnson, J. E.; Heck, A. J. R. *Angew. Chem., Int. Ed.* **2013**, *52*, 4020–4023.
- (244) Hernández, H.; Robinson, C. V. *Nat. Protoc.* **2007**, *2*, 715–726.
- (245) Benesch, J. L. P.; Ruotolo, B. T.; Sobott, F.; Wildgoose, J.; Gilbert, A.; Bateman, R.; Robinson, C. V. *Anal. Chem.* **2009**, *81*, 1270–1274.
- (246) Belov, M. E.; Damoc, E.; Denisov, E.; Compton, P. D.; Horning, S.; Makarov, A. A.; Kelleher, N. L. *Anal. Chem.* **2013**, *85*, 11163–11173.
- (247) Rose, R. J.; Damoc, E.; Denisov, E.; Makarov, A.; Heck, A. J. R. *Nat. Methods* **2012**, *9*, 1084–1086.
- (248) Li, H.; Wolff, J. J.; Van Orden, S. L.; Loo, J. A. *Anal. Chem.* **2014**, *86*, 317–320.
- (249) Yin, S.; Loo, J. A. *J. Am. Soc. Mass Spectrom.* **2010**, *21*, 899–907.
- (250) Clarke, D. J.; Murray, E.; Hupp, T.; Mackay, C. L.; Langridge-Smith, P. R. R. *J. Am. Soc. Mass Spectrom.* **2011**, *22*, 1432–1440.
- (251) Zhang, H.; Cui, W.; Wen, J.; Blankenship, R. E.; Gross, M. L. *Anal. Chem.* **2011**, *83*, 5598–5606.
- (252) Zhang, H.; Cui, W.; Gross, M. L. *Int. J. Mass Spectrom.* **2013**, *354–355*, 288–291.
- (253) Breuker, K.; Brüschweiler, S.; Tollinger, M. *Angew. Chem., Int. Ed.* **2011**, *50*, 873–877.
- (254) Li, H.; Wongkongkathep, P.; Van Orden, S. L.; Ogorzalek Loo, R. R.; Loo, J. A. *J. Am. Soc. Mass Spectrom.* **2014**, *25*, 2060–2068.
- (255) Lermyte, F.; Konijnenberg, A.; Williams, J. P.; Brown, J. M.; Valkenburg, D.; Sobott, F. *J. Am. Soc. Mass Spectrom.* **2014**, *25*, 343–350.
- (256) Zhang, Z.; Browne, S. J.; Vachet, R. W. *J. Am. Soc. Mass Spectrom.* **2014**, *25*, 604–613.
- (257) Lermyte, F.; Sobott, F. *Proteomics* **2015**, *15*, 2813–2822.
- (258) Canon, F.; Milosavljević, A. R.; van der Rest, G.; Réfrégiers, M.; Nahon, L.; Sarni-Manchado, P.; Cheynier, V.; Giuliani, A. *Angew. Chem., Int. Ed.* **2013**, *52*, 8377–8381.
- (259) Warnke, S.; Baldauf, C.; Bowers, M. T.; Pagel, K.; von Helden, G. *J. Am. Chem. Soc.* **2014**, *136*, 10308–10314.
- (260) Cammarata, M.; Lin, K.-Y.; Pruet, J.; Liu, H.-w.; Brodbelt, J. S. *Anal. Chem.* **2014**, *86*, 2534–2542.
- (261) O'Brien, J. P.; Li, W.; Zhang, Y.; Brodbelt, J. S. *J. Am. Chem. Soc.* **2014**, *136*, 12920–12928.
- (262) Cammarata, M.; Brodbelt, J. S. *Chemical Science* **2015**, *6*, 1324–1333.
- (263) Cammarata, M.; Thyer, R.; Rosenberg, J.; Ellington, A.; Brodbelt, J. S. *J. Am. Chem. Soc.* **2015**, *137*, 9128–9135.
- (264) Dyachenko, A.; Wang, G.; Belov, M.; Makarov, A.; de Jong, R. N.; van den Bremer, E. T.; Parren, P. P. W. H. I.; Heck, A. J. R. *Anal. Chem.* **2015**, *87*, 6095–6102.